Supporting Information

The Structural Basis of Sirtuin 6-Catalyzed Nucleosome Deacetylation

Zhipeng A. Wang,[†,‡,#] Jonathan W. Markert,[§,#] Samuel D. Whedon,[†,‡,#] Maheeshi Yapa Abeywardana,[†,‡] Kwangwoon Lee,[†,‡] Hanjie Jiang,[†,‡] Carolay Suarez,[†,‡] Hening Lin,[^] Lucas Farnung,[§,*] and Philip A. Cole.[†,‡,*]

[†] Division of Genetics, Department of Medicine, Brigham and Women's Hospital, Boston, MA, United States, 02115;

[‡] Department of Biological Chemistry and Molecular Pharmacology, Harvard Medical School, Boston, MA, United States, 02115;

[§] Department of Cell Biology, Blavatnik Institute, Harvard Medical School, Boston, MA 02115;

[^] Howard Hughes Medical Institute; Department of Chemistry and Chemical Biology, Cornell University, Ithaca, NY, United States, 14853;

# Equal contributors

* Corresponding authors: Lucas_Farnung@hms.harvard.edu; pacole@bwh.harvard.edu

Table of Contents

Design and cloning of Sirt6 mutants

His-Sirt6 plasmid was donated by Hening Lin lab (Kanamycin resistant). A TEV cleavage site was inserted between the His-tag and Sirt6 sequence. A N-terminal Cys was left in case for further chemical biology handling.

His-TEV-Cys-Sirt6 1-355 sequence (TEV site are underlined)

CATCATCATCATCATCACAGCAGCGGCCTGGTGCCGCGCGGCAGCCATgaaaacctgtattttcagtgcTC
GGTGAATTACGCGGCGGGGCTGTCGCCGTACGCGGACAAGGGCAAGTGCGGCCTCCCGGAG
ATCTTCGACCCCCCGGAGGAGCTGGAGCGGAAGGTGTGGGAACTGGCGAGGCTGGTCTGGC
AGTCTTCCAGTGTGGTGTTCCACACGGGTGCCGGCATCAGCACTGCCTCTGGCATCCCCGAC
TTCAGGGGTCCCCACGGAGTCTGGACCATGGAGGAGCGAGGTCTGGCCCCCAAGTTCGACA
CCACCTTTGAGAGCGCGCGGCCCACGCAGACCCACATGGCGCTGGTGCAGCTGGAGCGCGT
GGGCCTCCTCCGCTTCCTGGTCAGCCAGAACGTGGACGGGCTCCATGTGCGCTCAGGCTTCC
CCAGGGACAAACTGGCAGAGCTCCACGGGAACATGTTTGTGGAAGAATGTGCCAAGTGTAA
GACGCAGTACGTCCGAGACACAGTCGTGGGCACCATGGGCCTGAAGGCCACGGGCCGGCTC
TGCACCGTGGCTAAGGCAAGGGGGCTGCGAGCCTGCAGGGGAGAGCTGAGGGACACCATCC
TAGACTGGGAGGACTCCCTGCCCGACCGGGACCTGGCACTCGCCGATGAGGCCAGCAGGAA
CGCCGACCTGTCCATCACGCTGGGTACATCGCTGCAGATCCGGCCCAGCGGGAACCTGCCGC
TGGCTACCAAGCGCCGGGGAGGCCGCCTGGTCATCGTCAACCTGCAGCCCACCAAGCACGA
CCGCCATGCTGACCTCCGCATCCATGGCTACGTTGACGAGGTCATGACCCGGCTCATGAAGC
ACCTGGGGCTGGAGATCCCCGCCTGGGACGGCCCCCGTGTGCTGGAGAGGGCGCTGCCACC
CCTGCCCCGCCCGCCCACCCCCAAGCTGGAGCCCAAGGAGGAATCTCCCACCCGGATCAAC
GGCTCTATCCCCGCCGGCCCCAAGCAGGAGCCCTGCGCCCAGCACAACGGCTCAGAGCCCG
CCAGCCCCAAACGGGAGCGGCCCACCAGCCCTGCCCCCCACAGACCCCCCAAAAGGGTGAA
GGCCAAGGCGGTCCCCAGCTG

Primers:

0. QC-TEVCysS6-F:

5'-TGGTGCCGCGCGGCAGCCATGAAAACCTGTATTTTCAGTGCTCGGTGAATTACGCGGCGG

QC-TEVCysS6-R:

5'-CCGCCGCGTAATTCACCGAGCACTGAAAATACAGGTTTTCATGGCTGCCGCGCGGCACCA

1. Sirt6 R172A-F:

5'-gcgGGGCTGCGAGCCTGCAGGG

Sirt6 R172A-R:

5'-TGCCTTAGCCACGGTGCAGAGCC

2. Sirt6 R175A-F:

5'-gcgGCCTGCAGGGGAGAGCTGAGGG

Sirt6 R175A-R:

5'-CAGCCCCCTTGCCTTAGCCACGG

3. Sirt6 acidic patch-binding tetra-mutant-F:

5'-agcggcctgtgcgGGAGAGCTGAGGGACACCATCCTAGACTGG

Sirt6 acidic patch-binding tetra-mutant-R:

5'-aaacctgcagctgcAGCCACGGTGCAGAGCCGGCCCG

4. Sirt6 R231A/R232A-F:

5'-gcgGGAGGCCGCCTGGTCATCGTCAACC

Sirt6 R231A/R232A-R:

5'-cgcCTTGGTAGCCAGCGGCAGGTTCCCGC

5. Sirt6 R248A-F:
5'-gcgCATGCTGACCTCCGCATCCATGGC
Sirt6 R248A-R:
5'-GTCGTGCTTGGTGGGCTGCAGG

6. Sirt6 R205A-F:
5'-AACGCCGACCTGTCCATCACGCTGG
Sirt6 R205A-R:
5'-TGCGCTGGCCTCATCGGCGAG

His-TEV-Cys-Sirt6 sequence (TEV site are underlined)
HHHHHHSSGLVPRGSHENLYFQCSVNYAAGLSPYADKGKCGLPEIFDPPEELERKVWELARLV
WQSSSVVFHTGAGISTASGIPDFRGPHGVWTMEERGLAPKFDTTFESARPTQTHMALVQLERVG
LLRFLVSQNVDGLHVRSGFPRDKLAELHGNMFVEECAKCKTQYVRDTVVGTMGLKATGRLCT
VAKARGLRACRGELRDTILDWEDSLPDRDLALADEASRNADLSITLGTSLQIRPSGNLPLATKRR
GGRLVIVNLQPTKHDRHADLRIHGYVDEVMTRLMKHLGLEIPAWDGPRVLERALPPLPRPPTPK
LEPKEESPTRINGSIPAGPKQEPCAQHNGSEPASPKRERPTSPAPHRPPKRVKAKAVPS

Other mutations were done by one or several rounds of quick-change site directed mutagenesis. Each of the PCR products was purified by PCR cleanup kit (Zymo), treated with DpnI (New England Biolabs), and then transformed into DH5α *E. coli*. Single colonies were picked and let to grow overnight in 5 mL of Luria Bertani media (LB) supplemented with kanamycin (50 μg / mL), then pelleted (5 minutes, 4500 rcf, 4 ˚C). Plasmids were obtained from cell pellets by mini-prep (Plasmid Miniprep Classic, Zymo) and Sanger sequenced.

Sirt6(1-355) M1C/R172A amino acid sequence (R172A) (mutations are underlined, TEV cut site is **bolded**, His tag is *italicized*)
*HHHHHH*SSGLVPRGSH**ENLYFQC**SVNYAAGLSPYADKGKCGLPEIFDPPEELERKVWELARLV
WQSSSVVFHTGAGISTASGIPDFRGPHGVWTMEERGLAPKFDTTFESARPTQTHMALVQLERVG
LLRFLVSQNVDGLHVRSGFPRDKLAELHGNMFVEECAKCKTQYVRDTVVGTMGLKATGRLCT
VAKAAGLRACRGELRDTILDWEDSLPDRDLALADEASRNADLSITLGTSLQIRPSGNLPLATKRR
GGRLVIVNLQPTKHDRHADLRIHGYVDEVMTRLMKHLGLEIPAWDGPRVLERALPPLPRPPTPK
LEPKEESPTRINGSIPAGPKQEPCAQHNGSEPASPKRERPTSPAPHRPPKRVKAKAVPS

Sirt6(1-355) M1C/R175A amino acid sequence (Sirt6 R175A) (mutations are underlined, TEV cut site is **bolded**, His tag is *italicized*)
*HHHHHH*SSGLVPRGSH**ENLYFQC**SVNYAAGLSPYADKGKCGLPEIFDPPEELERKVWELARLV
WQSSSVVFHTGAGISTASGIPDFRGPHGVWTMEERGLAPKFDTTFESARPTQTHMALVQLERVG
LLRFLVSQNVDGLHVRSGFPRDKLAELHGNMFVEECAKCKTQYVRDTVVGTMGLKATGRLCT
VAKARGLAACRGELRDTILDWEDSLPDRDLALADEASRNADLSITLGTSLQIRPSGNLPLATKRR
GGRLVIVNLQPTKHDRHADLRIHGYVDEVMTRLMKHLGLEIPAWDGPRVLERALPPLPRPPTPK
LEPKEESPTRINGSIPAGPKQEPCAQHNGSEPASPKRERPTSPAPHRPPKRVKAKAVPS

Sirt6(1-355) M1C/K170A/R172A/R175A/R178A (Sirt6 acidic patch-binding tetra-mutant) amino acid sequence (mutations are underlined, TEV cut site is **bolded**, His tag is *italicized*)
*HHHHHH*SSGLVPRGSH**ENLYFQC**SVNYAAGLSPYADKGKCGLPEIFDPPEELERKVWELARLV
WQSSSVVFHTGAGISTASGIPDFRGPHGVWTMEERGLAPKFDTTFESARPTQTHMALVQLERVG
LLRFLVSQNVDGLHVRSGFPRDKLAELHGNMFVEECAKCKTQYVRDTVVGTMGLKATGRLCT
VAAAAGLAACAGELRDTILDWEDSLPDRDLALADEASRNADLSITLGTSLQIRPSGNLPLATKRR

GGRLVIVNLQPTKHDRHADLRIHGYVDEVMTRLMKHLGLEIPAWDGPRVLERALPPLPRPPTPK
LEPKEESPTRINGSIPAGPKQEPCAQHNGSEPASPKRERPTSPAPHRPPKRVKAKAVPS

Sirt6(1-355) M1C/R231A/R232A amino acid sequence (Sirt6 R2312232A) (mutations are underlined, TEV cut site is **bolded**, His tag is *italicized*)
*HHHHHH*SSGLVPRGSH**ENLYFQ**CSVNYAAGLSPYADKGKCGLPEIFDPPEELERKVWELARLV
WQSSSVVFHTGAGISTASGIPDFRGPHGVWTMEERGLAPKFDTTFESARPTQTHMALVQLERVG
LLRFLVSQNVDGLHVRSGFPRDKLAELHGNMFVEECAKCKTQYVRDTVVGTMGLKATGRLCT
VAKARGLRACRGELRDTILDWEDSLPDRDLALADEASRNADLSITLGTSLQIRPSGNLPLATKAA
GGRLVIVNLQPTKHDRHADLRIHGYVDEVMTRLMKHLGLEIPAWDGPRVLERALPPLPRPPTPK
LEPKEESPTRINGSIPAGPKQEPCAQHNGSEPASPKRERPTSPAPHRPPKRVKAKAVPS

Sirt6(1-355) M1C/R248A amino acid sequence (Sirt6 R248A) (mutations are underlined, TEV cut site is **bolded**, His tag is *italicized*)
*HHHHHH*SSGLVPRGSH**ENLYFQ**CSVNYAAGLSPYADKGKCGLPEIFDPPEELERKVWELARLV
WQSSSVVFHTGAGISTASGIPDFRGPHGVWTMEERGLAPKFDTTFESARPTQTHMALVQLERVG
LLRFLVSQNVDGLHVRSGFPRDKLAELHGNMFVEECAKCKTQYVRDTVVGTMGLKATGRLCT
VAKARGLRACRGELRDTILDWEDSLPDRDLALADEASRNADLSITLGTSLQIRPSGNLPLATKRR
GGRLVIVNLQPTKHDAHADLRIHGYVDEVMTRLMKHLGLEIPAWDGPRVLERALPPLPRPPTPK
LEPKEESPTRINGSIPAGPKQEPCAQHNGSEPASPKRERPTSPAPHRPPKRVKAKAVPS

Sirt6(1-355) M1C/R205A/ R231A/R232A/R248A (Sirt6 DNA-binding tetra-mutant) amino acid sequence (mutations are underlined, TEV cut site is **bolded**, His tag is *italicized*)
*HHHHHH*SSGLVPRGSH**ENLYFQ**CSVNYAAGLSPYADKGKCGLPEIFDPPEELERKVWELARLV
WQSSSVVFHTGAGISTASGIPDFRGPHGVWTMEERGLAPKFDTTFESARPTQTHMALVQLERVG
LLRFLVSQNVDGLHVRSGFPRDKLAELHGNMFVEECAKCKTQYVRDTVVGTMGLKATGRLCT
VAKARGLRACRGELRDTILDWEDSLPDRDLALADEASANADLSITLGTSLQIRPSGNLPLATKAA
GGRLVIVNLQPTKHDAHADLRIHGYVDEVMTRLMKHLGLEIPAWDGPRVLERALPPLPRPPTPK
LEPKEESPTRINGSIPAGPKQEPCAQHNGSEPASPKRERPTSPAPHRPPKRVKAKAVPS

Expression and purification of His-Sirt6, WT Sirt6 and Sirt6 mutants
All Sirt6 constructs were transformed into LOBSTR *E. coli* strain derived from Rosetta (DE3). Single colony was picked to let to grow in 5 mL Luria Bertani (LB) seed culture for overnight (12-16 hr) with constant shaking (200 rpm). Then 1 L of LB media supplemented with 50 mg/L kanamycin was inoculated with 10 mL from a starter culture. The 1 L LB culture was grown at 37 ˚C, 200 rpm for about 3.5 h to an OD_{600} of 0.6, and the overexpression was induced with the addition of IPTG to 0.5 mM. Then the temperature was brought down to 25 ˚C, and the culture grew for a further 18 hr at 25 ˚C, 200 rpm. The culture was pelleted by centrifugation at 4,000 × g, 4 ˚C, and the supernatant was removed. Cell pellets were stored at -80 ˚C overnight before being processed. The cell pellet was resuspended in 30 mL ice cold lysis buffer (20 mM Tris, 500 mM NaCl, 20 mM imidazole, pH 7.5) and then lysed by passing through a French pressure cell three times. Lysate was centrifuged at 13,000 × g, 4 ˚C, and the lysate supernatant was applied to pre-equilibrated Ni-NTA resin (2 mL resin bed volume / 1 L culture). After incubating for 1 h at 4 ˚C, the flow-through was removed by passing the column by gravity at a moderate drip rate. The resin bed was first washed with 10 column volumes of wash buffer (20 mM Tris, 500 mM NaCl, 50 mM imidazole, 0.5 mM TCEP, pH 7.5), and then washed with 25 column volumes of high-salt wash buffer (20 mM Tris, 2 M NaCl, 20 mM imidazole, pH 7.5), followed by 10 column volumes of elution buffer (20 mM Tris, 500 mM NaCl, 200 mM imidazole, 0.5 mM TCEP, pH 7.5). The elution was concentrated by spin concentrator (Amicon, 10 kDa MWCO, 4,000 rpm, 4 ˚C), before overnight dialysis at 4 ˚C (dialysis buffer: 20 mM Tris, 150 mM NaCl, 20 mM imidazole, 0.5 mM TCEP, pH 7.5). For WT-Sirt6 and all Sirt6 mutants, ~ 1 mL TEV protease (~ 1 mg/mL) was mixed with the elution before dialysis. The dialyzed sample was re-applied to pre-equilibrated Ni-NTA resin. After incubating for 1 h at 4 ˚C, the flow-through was collected

by gravity at a moderate drip rate. After diluting with 10 mL Heparin buffer A (50 mM Tris, 150 mM NaCl, 5 % glycerol, 0.5 mM TCEP, pH 7.5), the flow-through was concentrated by spin concentrator (Amicon, 10 kDa MWCO, 4,000 rpm, 4 ˚C), and then applied to Heparin column (1 mL, Cytiva, #17040601), and eluted with a linear gradient from 0-50 % Heparin buffer B (50 mM Tris, 2000 mM NaCl, 5 % glycerol, 0.5 mM TCEP, pH 7.5) over 20 column volumn (CV) at a flow rate of 0.6 mL/min (Figure S3A). Elution fractions were checked by SDS-PAGE (6-20 %, Biorad), and the pure fractions were collected and concentrated. This was further purified by size exclusion using a Superdex200 column (GE, #28-9909-44) with Superdex running buffer (50 mM Tris, 150 mM NaCl, 0.5 mM TCEP, pH 7.5) (Figure S3B). Elution fractions were checked by SDS-PAGE, and the pure fractions were combined and concentrated to ~200 µL, or a final concentration of ~40 µM. (Figure S3C). SDS-PAGE was used for densitometry and quality check for WT Sirt6 and all the Sirt6 mutants. WT Sirt6 was characterized by ESI-MS (Q Exactive, Thermo Scientific) and deconvoluted using UniDec[1] (Figure S1). WT Sirt6 and all Sirt6 mutants were aliquoted and flash-frozen in liquid nitrogen, then stored at -80 ˚C.
WT Sirt6 calculated average mass for $C_{1718}H_{2770}N_{514}O_{503}S_{13}$ [M]+: 39090.82 Da; Observed: 39089.0 Da

Expression of TEV protease
The pET-6xHis-TEV plasmid was transformed into Rosetta (DE3) pLysS Codon Plus *E. coli* competent cells for recombinant protein expression. The transformed cells were cultured from fresh LB plates into 2xYT medium to optimal cell density at OD_{600} = 0.6. Then 0.5 mM isopropyl thiogalactoside (IPTG) was added to induce protein expression at 20 ˚C for 20 h. After french press lysis, Ni-NTA resin was used for the purification in a buffer containing 25 mM HEPES, pH 7.8, 500 mM NaCl, 25 mM imidazole, and 1mM TCEP. After washing and gradually increasing the imidazole concentration for elution, the eluted fractions were analyzed by Coomassie Blue–stained SDS-PAGE and fractions containing high purity protein were combined. Then the combined fractions were dialyzed against a buffer containing 25 mM HEPES, pH 7.8, 500 mM NaCl, and 1 mM TCEP at 4 ˚C to gradually remove imidazole. After dialysis, glycerol was added to 20 % (v/v) to the protein and the protein was concentrated to 1mg/mL, determined by SDS-PAGE gel with BSA standards. The purified proteins were aliquoted, flash-frozen, and stored at -80 ˚C.

Expression of sortase mutants
Sortase mutants were derived from *S. aureus* sortase A (Srt A). The previously reported F40 sortase has altered sorting motif preference for APXTG, while W4 recognizes the sequence HPXTG. DNA encoding S. aureus Srt A (60-206) (from Dirk Schwarzer lab) was cloned into pET21 vector (Ampicillin resistant). W4 was derived from F40 by sequential site-directed mutagenesis, as previously described.

F40 amino acid sequence (mutations distinguishing F40 from Srt A are underlined, His tag is *italicized*)
MQAKPQIPKDKSKVAGYIEIPDADIKEPVYPGPATPEQLNRGVSFAEENESLDDQNISIAGHTFIDR
PNYQFTNLKAAKMGSMVYFKVGNETRKYKMTSIRDVKPQDVGMHLAEKGKDKQLTLITCDDY
NEKTGVWEKRKIFVATEVKLE*HHHHHH*

W4 amino acid sequence (mutations distinguishing W4 from Srt A are underlined, His tag is *italicized*)
MQAKPQIPKDKSKVAGYIEIPDADIKEPVYPGPATSEQLNRGVSFAKENQSLDDQNISIAGHTFIG
RPNYQFTNLKAAKMGSMVYFKVGNETRKYKMTSIRNVKPQDVGMHLAEKGKDKQLTLITCDD
LNRETGVWETRKIFVATEVKLE*HHHHHH*

Constructs were transformed into BL21-CodonPlus (DE3) RIPL *E. coli*. Starter cultures were grown overnight (12-16 hr, 37 ˚C, 200 rpm) in 50 mL of Luria Bertani (LB) media supplemented with 100 mg/L ampicillin from scrapings of a frozen cell stock. Subsequently 1 L LB cultures with 100 mg/L ampicillin were inoculated with 10 mL of starter culture and grown to an OD_{600} of 0.3-0.5 (37 ˚C, 200 rpm). Prior to induction the temperature was reduced to 25-30 ˚C. At an OD_{600} of 0.5-0.8 overexpression was induced with the addition of IPTG to 0.3 mM. Cells were grown for a further 3 hr, then cultures were pelleted by centrifugation (5,000 × g, 4 ˚C). Cell pellets were either stored at -80 ˚C, or immediately processed. Cell

pellets were resuspended in 5 pellet volumes ice cold lysis buffer (20 mM Tris, pH 7.5, 0.1% Triton X-100), made uniform by dounce homogenizer, and lysed by three passages through a microfluidizer. Lysates were clarified by centrifugation (13,000 x g, 4 ˚C), and lysate supernatants were applied to Ni-NTA resin (2.5 mL resin bed volume / 1 L culture) pre-equilibrated with cold lysis buffer. Resin was washed with 10 column volumes of lysis buffer, then 20 volumes of wash buffer (20 mM Tris, pH 7.5, 500 mM NaCl), and then 10 volumes of lysis buffer supplemented with 5% elution buffer (20 mM Tris, pH 7.5, 400 mM imidazole). Protein was eluted in five to ten fractions of elution buffer, each of 2 column volumes. Elution fractions were checked by SDS-PAGE (15%) and pooled. Purified protein was dialyzed three times against 40 volumes of 50 mM Tris, pH 7.5, 150 mM NaCl, 5 mM $CaCl_2$ at 4 ˚C. Protein was then concentrated by spin concentrator (Amicon, 10 kDa MWCO, 4,000 rpm, 4 ˚C) to 1-3 mM by the absorbance at 280 nm measured by nanodrop (Thales).

General peptide synthesis methods

All peptides were synthesized by Fmoc-based solid phase peptide synthesis with Rink Amide AM resin (EMD Millipore). Syntheses were performed using a Prelude automated peptide synthesizer (Gyros Protein Technologies) using the following deprotection & coupling cycle for a 0.2 mmol scale synthesis: 5 mL of 20% piperidine in DMF was added to the reaction vessel and mixed for 10 min, the vessel was drained, and a second identical deprotection followed; 4 mL of DMF was added to the reaction vessel and mixed for 30 sec, the vessel was drained, and five more washes followed alternating solvent delivery from the top and bottom of the reaction vessel; 0.8 mmol (4 eq) Fmoc-amino acid in 4 mL DMF, and 0.75 mmol (3.75 eq) HATU and 1.6 mmol (8 eq) N-methylmorpholine (NMM) in 4 mL DMF were sequentially added to the reaction vessel and mixed for 90 min, followed one wash with 4 mL DMF (as before), and a second identical coupling. After the final amino acid coupling peptides were N-terminally deprotected, as described above, and the resin was sequentially washed with DMF and dichloromethane (DCM), then dried under vacuum. Cleavage of the peptide from the resin and removal of the side chain protecting groups was accomplished by addition of Reagent B (5 % water, 5 % phenol, 2.5 % triisopropyl silane (TIPS), 87.5 % trifluoroacetic acid (TFA)) and 90-180 minutes of agitation. Resin was removed by filtration, and crude peptide was preciptated by adding 10 volumes of ice-cold diethyl ether. The precipitate was washed a further two times with ice-cold diethyl ether before drying under a stream of nitrogen. Crude peptides were purified by reverse-phase HPLC with either a C18 semi-preparative column (Varian Dynamax Microsorb 100, 250×21.4 mm) or a C8 semi-prep column (Varian Dynamax Microsorb 100, 250×21.4mm). H3(1-34) peptides were purified using the C18 column and a linear gradient from 7 % CH_3CN/0.05 % TFA to 30 % CH_3CN/0.05 % TFA over 30 min at a flow rate of 10 mL/min. H2B(4-52) TOG peptides were purified using the C8 column and a linear gradient from 25 % CH_3CN/0.05 % TFA to 55 % CH_3CN/0.05 % TFA over 30 min, at a flow rate of 10 mL/min. Pure fractions were determined by MALDI-TOF MS (Dana Farber Cancer Institute Molecular Biology Core Facilities, 4800 MALDI TOF/TOF, Applied Biosystems/MDS Sciex) or ESI-MS (Q Exactive, Thermo Scientific), then combined, lyophilized and stored at -80 ˚C as dry powders, or concentrated stock solutions. Pooled, purified materials were characterized by ESI-MS (Q Exactive, Thermo Scientific) and deconvoluted using UniDec.[1]

Incorporating depsipeptide Fmoc-Thr(OtBu)-glycolic acid (TOG) into peptides

The synthesis of TOG was done as described before[2]. After the coupling of the first Gly, the second amino acid coupled in each H3 and H2B peptide was the depsipeptide TOG, which was hand coupled overnight with 0.4 mmol (2 eq) TOG, 0.36 mmol (1.8 eq) HATU, and 0.8 mmol (4 eq) DIPEA. No capping step was used, and subsequent couplings followed the general protocol.

Incorporating N-thioacetyl (Sac) into peptide

Fmoc-Lys(alloc)-OH was installed using the standard conditions described above into H3K9 site as H3K9alloc 1-34 TOG. To facilitate side-chain derivatization, Boc-Ala was used instead of Fmoc-Ala at the 1 position in the H3 peptide. Side chain deprotection was conducted as previously reported[2]. Briefly,

vacuum dried $Pd(PPh_3)_4$ (0.35 eq relative to resin; Strem Chemicals cat# 46-2150) was dissolved in anhydrous dichloromethane (Sigma-Aldrich cat# 270997), and combined with phenylsilane (20 eq relative to resin; Chem-Impex cat# 31483). This solution was added to the peptide resin and mixed by bubbling with nitrogen for 60 minutes. The reaction solution was drained, and the deprotection was repeated once more. The resin was then extensively washed with dichloromethane and DMF, however it unavoidably retained a darker color after Pd deprotection.

Thioacetylation of the the free amino group of K9 was accomplished with ethyl dithioacetate. To the resin was added ethyl dithioacetate (20 eq relative to resin; Sigma-Aldrich #358851-1ML) and *N,N*-diisopropylethylamine (DIPEA, 40 eq; Sigma-Aldrich cat# 125806). This mixture was placed on an end-over-end rotator for 8 h, after which the reagent was removed by vacuum and fresh reagent was added. The reaction was repeated for a total of 3 times. After carefully washing, Fmoc-Cl (10 eq, Sigma-Aldrich #23186-1G) was added together with DIPEA (20 eq) to cap unreacted lysine, and the mixture was placed on an end-over-end rotator for 18 h. Peptide cleavage, precipitation and purification followed the general protocol. Pooled, purified materials were characterized by ESI-MS (Q Exactive, Thermo Scientific) and deconvoluted using UniDec[1] (Figure S2A).

Sequence: ARTKQTARK(Sac)STGGKAPRKQLATKAARKSAPA-TOG-G

H3K9Sac 1-34 TOG $[M]^+$ calculated for $C_{146}H_{263}N_{55}O_{44}S$ as 3507.96 Da; Observed: 3508.8 Da

Incorporating N-methyl thiourea (MTU) into peptide

N-terminal Boc protection and alloc deprotection was performed as described in the above N-thioacetyl incorporation protocol. Methyl isothiocyanate (1 eq relative to resin; Sigma-Aldrich # 112771) in dry dichloromethane was added to the peptide resin. DIPEA was dried by passing over a silica plug column, and then added to the peptide resin (1 eq relative to resin). This mixture was placed on an end-over-end rotator. After 60 hours the reaction was judged to have stopped at ~60% conversion (RP-HPLC peak area). Peptide cleavage, precipitation and purification followed the general protocol. Pooled, purified materials were characterized by ESI-MS (Q Exactive, Thermo Scientific) and deconvoluted using UniDec[1] (Figure S2B).

Sequence: ARTKQTARK(MTU)STGGKAPRKQLATKAARKSAPA-TOG-G

H3K9MTU 1-314 TOG $[M]^+$ calculated for $C_{146}H_{263}N_{55}O_{44}S$ as 3522.98 Da, observed at 3521.9 Da

Expression of histone H2A, H2B, H3, H4, gH3 and C-H2B

Wild type (WT) *Xenopus laevis* core histones H2A, H2B, H3, and H4,[3] together with gH3 (aa33-135) and C-H2B (aa53-125) were expressed and purified as previously reported. Both H3 and gH3 constructs carry a C110A mutation, which is widely used in both nucleosome chemical biology and nucleosome structural studies.[4] Generally, histone expression was freshly transformed *E. coli* Rosetta (DE3) pLysS, which were plated on LB agar plates supplemented with ampicillin (100 μg/mL). After 12-16 h at 37 ˚C, a single colony was used to inoculate a 50 mL starter culture of LB media supplemented with 100 mg/L ampicillin, and grown at 37 ˚C (200 rpm). After a further 12-16 hours 10 mL of starter culture was used to inoculate 1 L of LB media supplemented with 100 mg/L ampicillin. This culture was grown at 37 ˚C (200 rpm) until the OD_{600} was 0.6. Expression was induced with 0.5 mM IPTG at 37 ˚C for 2-4 hr. Cells were harvested by centrifugation at 4,000 rpm for 15 min. Cell pellets were resuspended in histone lysis buffer (50 mM Tris-HCl at pH 7.5, 100 mM NaCl, 1 mM EDTA, 5 mM 2-mercaptoethanol (BME), with 1% Triton X-100). Resuspended cell pellets were made uniform by dounce homogenizer and lysed by three passages through a microfluidizer. Lysed cells were centrifuged for 30 min at 15,000 g, 4 ˚C, and the supernatant was discarded. The pellet (inclusion bodies) was then washed by resuspending and vortexing five times with histone wash buffer (50 mM Tris-HCl at pH 7.5, 100 mM NaCl, 1 mM EDTA). After the removal of all the supernatants, the pellets were resuspended in ion exchange (IEX) buffer A (7 M urea, 10 mM Tris pH 7.8, 1 mM EDTA, and 5 mM BME) with vortexing, stirring and sonication to maximize protein solublization (*Note: these resuspended samples are not completely soluble, and generally contain translucent amber particulate)*. The resuspension is centrifuged for 30 min at 15,000 g, 4 ˚C, and the supernatant is loaded onto passed over connected, pre-packed Q and SP columns (5 mL HiTrap Q HP and 5 mL HiTrap SP HP,

GE healthcare). IEX buffer A containing 100 mM NaCl was used to equilibrate and wash both Q and SP columns. After the Q column is washed with 5-10 column volumes of IEX A it is detached from the SP column, and the histone is isolated by gradient wash and elution of SP column (100 mM - 500 mM NaCl in IEX A). All fractions are evaluated by SDS-PAGE (15%), and those containing histone are combined and dialyzed three times against pre-chilled, ice-cold water with 0.05% TFA, then concentrated (Amicon Ultra 15 mL, 10 kDa MWCO, EMD Millipore), aliquoted in 3 mg portions, flash-frozen, lyophilized to dryness and stored at -80 ˚C until usage. C-H2B samples were re-dissolved in denaturant and further purified by reverse-phase HPLC with a C8 semi-preparative column (Varian Dynamax Microsorb 100, 250×21.4 mm). A linear gradient from 30 % CH_3CN/0.05 % TFA to 50 % CH_3CN/0.05 % TFA over 30 min at a flow rate of 10 mL/min was used for C-H2B purification to reach a final > 95 % purity by Coomassie stained SDS-PAGE. The combined C-H2B solution was then lyophilized to dryness and stored at -80 ˚C until usage.

H2A:
SGRGKQGGKTRAKAKTRSSRAGLQFPVGRVHRLLRKGNYAERVGAGAPVYLAAVLEYLTAEIL
ELAGNAARDNKKTRIIPRHLQLAVRNDEELNKLLGRVTIAQGGVLPNIQSVLLPKKTESSKSAKS
K

H2B:
AKSAPAPKKGSKKAVTKTQKKDGKKRRKTRKESYAIYVYKVLKQVHPDTGISSKAMSIMNSFV
NDVFERIAGEASRLAHYNKRSTITSREIQTAVRLLLPGELAKHAVSEGTKAVTKYTSAK

H3:
ARTKQTARKSTGGKAPRKQLATKAARKSAPATGGVKKPHRYRPGTVALREIRRYQKSTELLIRK
LPFQRLVREIAQDFKTDLRFQSSAVMALQEASEAYLVALFEDTNLAAIHAKRVTIMPKDIQLARR
IRGERA

H4:
SGRGKGGKGLGKGGAKRHRKVLRDNIQGITKPAIRRLARRGGVKRISGLIYEETRGVLKVFLEN
VIRDAVTYTEHAKRKTVTAMDVVYALKRQGRTLYGFGG

F40 sortase-catalyzed histone H3 semisynthesis

Histone H3 semisynthesis with F40 followed a previously reported protocol.[5] Briefly, dried gH3 is resuspended in ice cold water with gentle pipetting, and used for ligation within 72 hours, after which aggregation limits ligation efficiency. Lyophilized peptide is resuspended to 20 mM in ice cold water. Peptide (2 mM) and gH3 (0.2 mM) are combined in ligation buffer (40 mM PIPES pH 7.0, 5 mM CaCl2, 1 mM DTT) and the pH is adjusted to 7.0 with concentrated PIPES (400 mM PIPES pH 7.5), then F40 sortase is added (0.2 mM), and the reaction is placed in a 37 ˚C incubator overnight. The insoluble fraction contains the bulk of the product, and as such is separated from soluble peptide and sortase by centrifugation (3 min at 21,100 rcf). The pelleted solid is dissolved in ion exchange (IEX) buffer A (7 M urea, 10 mM Tris pH 7.8, 1 mM EDTA, and 5 mM BME) with vortexing and sonication, then loaded on a pre-equilibrated SP column (1 mL HiTrap SP HP, Cytiva) at 1 mL / min using a peristaltic pump (Pharmacia Biotech). The column is washed with 120 mM NaCl in IEX A for >20 column volumes, followed by sequential 5 column volume washes in which the concentration of NaCl is stepped up by 10 mM per wash (130 mM, 140 mM, 150 mM, etc.) until 200 mM NaCl is reached. The bulk of the product can be eluted in 250 mM and 300 mM NaCl fractions of 5-10 column volumes each. Washes and fractions are checked by SDS-PAGE (15%), and pure fractions are combined and dialyzed three times against pre-chilled, ice-cold water with 0.05% TFA, then lyophilized. Pooled, purified materials were characterized by ESI-MS (Q Exactive, Thermo Scientific) and deconvoluted using UniDec (Figure S2C,D, some data were shown before[5]).

WT-H3: $[M]^+$ calculated as m/z 15238.8, observed as m/z 15238.0;
gH3: $[M]^+$ calculated as m/z 11918. 8, observed as m/z 11918.0;
H3K9ac: $[M]^+$ calculated as m/z 15280.6, observed as m/z 15280.1;
H3K9Sac: $[M]^+$ calculated as m/z 15296.71 Da; Observed: 15296.5;
H3K9MTU: $[M]^+$ calculated as m/z 15311.7, observed as m/z 15311.2;
H3K14ac: $[M]^+$ calculated as m/z 15280.6, observed as m/z 15280.2;

H3K18ac: $[M]^+$ calculated as m/z 15280.6, observed as m/z 15280.1;
H3K23ac: $[M]^+$ calculated as m/z 15280.6, observed as m/z 15280.0;
H3K27ac: $[M]^+$ calculated as m/z 15280.6, observed as m/z 15279.8;

W4 sortase-catalyzed histone H2B semisynthesis

H2B semisynthesis by W4 sortase was done following a similar protocol as reported for F40 sortase catalyzed H3 semisynthesis.[5] The modified histone H2B N-terminal peptide (H2B 4-52 TOG) was prepared as a 5 mM stock solution, and the C-H2B (53-125) was prepared as a 1 mM stock solution. If necessary, both solutions were centrifuged to remove any precipitate. With the optimized condition tested by small scale (20 μL), large scale (~5 mL) W4 sortase-catalyzed H2B semisynthesis reaction was then carried out. H2B 4-52 TOG (~1 mM) and C-H2B (~0.1 mM) were added to a sortase reaction buffer (20 mM PIPES at pH 7.5, 1 mM DTT, without the addition of 5 mM $CaCl_2$), and mixed well. After being initiated by the addition of W4 sortase (to final ~500 mM), the ligation reaction was incubated at 37 ˚C for 12 hr. The reaction produces substantial precipitate, which contains most of the H2B product, C-H2B with some W4 sortase, and could be isolated from the supernatant by centrifugation. The precipitate was then dissolved in 1 mL IEX buffer A (7 M urea, 10 mM Tris at pH 7.8, 1 mM EDTA and 5 mM BME). The combined solution was purified by reverse-phase HPLC with a C8 semi-prep column. These product fractions containing some C-H2B were carefully pooled and lyophilized until dry. The dry powder was then dissolved in 10 % CH_3CN/ 0.05% TFA in H2O/0.05 % TFA, and repurified by reverse-phase HPLC with a C18 analytic column (Agilent, Eclipse XDB-C18, 4.6×250 mm) with a linear gradient from 30 % CH_3CN/0.05 % TFA to 50 % CH_3CN/0.05 % TFA over 30 min at a flow rate of 1 mL/min. The collected fractions were then characterized by MALDI-TOF MS and pooled, lyophilized to powder, and stored at -80 ˚C. H2BK20ac and H2BK46ac were characterized by ESI-MS (LTQ Orbitrap, Thermo Q Exactive), while C-H2B, H2BK11ac, H2BK12ac, were characterized by MALDI-TOF (Dana Farber Cancer Institute Molecular Biology Core Facilities, 4800 MALDI TOF/TOF, Applied Biosystems/MDS Sciex) (data were shown before[2]).
C-H2B: $[M + H]^+$ calculated as m/z 7940.1, observed as m/z 7939.5;
H2BK11ac: $[M + H]^+$ calculated as m/z 13536.7, observed as m/z 13541.2;
H2BK12ac: $[M + H]^+$ calculated as m/z 13536.7, observed as m/z 13538.6;
H2BK20ac: $[M]^+$ calculated as m/z 13535.7, deconvolution as m/z 13537.8;
H2BK46ac: $[M]^+$ calculated as m/z 13535.7, deconvolution as m/z 13537.9;

147 and 185 bp DNA isolation

Preparation of 146 and 185 bp Widom 601 DNA was as previously reported[6]. Briefly, scrapings from a frozen cell stock were used to inoculate a 50 mL starter culture of LB media supplemented with 50 mg/L kanamycin, and grown at 37 ˚C (200 rpm) for 12-16 h. From this starter culture 10 mL was used to inoculate 1 L of CircleGrow media supplemented with 50 mg/L kanamycin. The 1 L culture was grown for a 24-30 h at 37 ˚C (200 rpm). Cells were harvested by centrifugation at 4,000 rpm for 15 min. Cell pellets were resuspended in 10 mM Tris pH 7.5, 10 mM EDTA (10 mL / g wet cell pellet mass) with vigorous mixing. Cells were lysed with lysozyme powder (10 mg powder / 1 mL lysozyme solution, Sigma-Aldrich cat# 62971) dissolved in 10 mM Tris pH 7.5, 10 mM EDTA (5 mL lysis solution / g wet cell pellet mass) and vigorously shaken, but not vortexed. The suspension became very viscous, taking on an appearance like wet dough. To this suspension was added 0.2 M sodium hydroxide (Chem-Impex cat# 30056) with 1% sodium dodecyl sulfate (Amresco cat# M107) (15 mL / g wet cell pellet weight), followed by vigorous shaking, but not vortexing. After 5 minutes of lysis the mixture was neutralized for a further 5 minutes with 1.5 M potassium acetate in 1.5 M acetic acid (12 mL / g wet cell pellet weight), followed by vigorous shaking. Insoluble material was pelleted by centrifugation at 4,000 rpm for 20 min. Any remaining insoluble material was removed by filtering over a glass fritted column. The solution was combined with 0.6 volumes of isopropanol, mixed by inverting, and allowed to stand for 5 minutes. The samples were pelleted by centrifugation at 4,000 rpm for 15 min, and the supernatant was discarded. The pellets were resuspended by pipetting in 10 mM Tris pH 7.5, 10 mM EDTA (15 mL / g wet cell pellet weight), then combined with

1 volume ice cold 5 M lithium chloride and kept for 5 minutes on ice. Insoluble material was removed by centrifugation at 4,000 rpm for 15 min, and the pellet was discarded. The supernatant was combined with 0.6 volumes of isopropanol, mixed by inverting and allowed to stand for 5 minutes. The samples were pelleted by centrifugation at 4,000 rpm for 15 min, and the supernatant was discarded. The pellets were resuspended by pipetting in 10 mM Tris pH 7.5, 1 mM EDTA (10 mL / g wet cell pellet weight), and heat treated RNAse A was added (0.005 volumes of 10 mg/mL stock) and the solution was incubated for 15 min at room temperature. The solution was combined with 3 volumes of isopropanol, mixed by inverting, allowed to stand for 5 minutes, and plasmid DNA was pelleted by centrifugation at 4,000 rpm for 10 min. Pellets were air dried and dissolved in 50 mM Tris pH 8.0, 1 mM EDTA (~40 mg plasmid DNA / 1 L culture). Dissolved plasmid DNA was combined with 10× rCutSmart buffer (NEB) and EcoRV (45 units / 1 mg plasmid DNA, NEB), and the pH was confirmed to be > 7.8 before incubating overnight at 37 ˚C with constant mixing. Digestion was checked by 1.5% Agarose TAE gel, and judged to have reached completion when the only observed bands were vector backbone (2.5-kbp) and single copy Widom 601 fragments (100-200 bp). The crude digest was diluted 10-fold with 10 mM Tris pH 7.5, 1 mM EDTA and loaded onto a 5 mL Q column (Cytiva) at a flow rate of 1 mL / min. The absorbance at 260 nm and 280 nm were monitored during column washing and elution. Washes with 200 mM NaCl in 10 mM Tris pH 7.5, 1 mM EDTA, then 600 mM NaCl in 10 mM Tris pH 7.5, 1 mM EDTA remove protein components.The product elutes at 700 mM NaCl in 10 mM Tris pH 7.5, 1 mM EDTA, while the vector backbone elutes at 800 mM NaCl in 10 mM Tris pH 7.5, 1 mM EDTA. The elution fractions were concentrated to 1 mg / mL by 260 nm absorbance and checked by 1.5% agarose/TAE gel before storing at -20 ˚C (data not shown).

DNA sequence:
185 bp DNA:
5'-
ATCGCTGTTCAATACATGCACAGGATGTATATATCTGACACGTGCCTGGAGACTAGGGAGTA
ATCCCCTTGGCGGTTAAAACGCGGGGGACAGCGCGTACGTGCGTTTAAGCGGTGCTAGAGCT
GTCTACGACCAATTGAGCGGCCTCGGCACCGGGATTCTCCAGGGCGGCCGCGTATAGGGAT-
3'
147 bp DNA:
5'-
CTGGAGAATCCCGGTGCCGAGGCCGCTCAATTGGTCGTAGACAGCTCTAGCACCGCTTAAAC
GCACGTACGCGCTGTCCCCCGCGTTTTAACCGCCAAGGGGATTACTCCCTAGTCTCCAGGCA
CGTGTCAGATATATACATCCTGT-3'

Octamer refolding and nucleosome reconstitution
In vitro octamer refolding and nucleosome assembly were carried out as previously reported.[7] Briefly, all four histone proteins (H2A, H2B, H3 and H4) were dissolved in denaturing buffer (7 M guanidine, 20 mM Tris-HCl at pH 7.5 and 10 mM DTT) with gentle mixing, then allowed to stand for ~30 min and quantified by 280 nm absorbance (nanodrop). Octamer preparations containing acylated H3 were mixed in a 1.2 : 1.2 : 1 : 1.1 ratio of H2A:H2B:H3ac:H4, such that the final protein concentration was ~1 mg/mL. Octamer preparations containing acylated H2B were mixed in a 1.1 : 1 : 0.9 : 0.9 ratio of H2A:H2Bac:H3:H4, such that the final protein concentration was ~1 mg/mL. The histone solution was then dialyzed (10 kDa molecular weight cutoff (MWCO) cassette, Slide-a-lyzer) against high salt octamer refolding buffer (20 mM Tris at pH 7.5, 2.0 M NaCl, 1 mM EDTA and 5 mM BME) three times at 4 ˚C. Crude octamers were concentrated (10 kDa MWCO, Amicon Ultra 0.5 mL, EMD Millipore) at 4 ˚C and purified by size exclusion FPLC (AKTApurifier, GE Healthcare) using a Superdex 200 10/300 GL column (GE Healthcare) with octamer refolding buffer as the mobile phase. Purified octamer was mixed with 147 bp Widom 601 DNA in 1:1 molar ratio, or with 185 bp Widom 601 DNA in a 1.2:1 molar ratio (octamer:DNA) in high salt buffer (10 mM Tris at pH 7.5, 2.0 M KCl, 1 mM EDTA and 1 mM DTT) with a final concentration of 6 μM octamer. A Minipuls two channel peristaltic pump (Gilson) was used to continuously add low salt buffer (10 mM Tris at pH 7.5, 250 mM KCl, 1 mM EDTA and 1 mM DTT) to the dialysis chamber, while

simultaneously removing buffer from the chamber. Buffers were transferred at a rate of ~1 mL/min over a period of 33-48 hours. The crude nucleosomes were purified by HPLC (Waters, 1525 binary pump, 2489 UV-Vis detector) with a TSKgel DEAE-5PW ion exchange column (TOSOH Bioscience, #83W-00096C) to remove free DNA. Mobile phase buffers were A TES250 (10 mM Tris pH 7.5, 250 mM KCl, 0.5 mM EDTA) and B TES600 (10 mM Tris pH 7.5, 600 mM KCl, 0.5 mM EDTA). The purification gradient was 0 % B for 4 min, followed by a linear gradient from 25 % to 75 % B over 30 min at 1 mL/ min flow rate. The fractions containing nucleosome products were immediately diluted with one volume of TCS Buffer (20 mM Tris at pH 7.5 and 1 mM DTT), then concentrated (10 kDa MWCO Amicon Ultra 4 mL, EMD Millipore) at 4 ˚C, and dialyzed three times against TCS buffer. Nucleosome samples intended for long-term storage were dialyzed against storage buffer (10 mM Tris pH 7.5, 25 mM NaCl, 1 mM DTT, 20% glycerol). Dialyzed nucleosomes were concentrated to 1-5 mM (Amicon Ultra 4 mL, 10 kDa MWCO, EMD Millipore), and analyzed by native 4-20 % TBE gels (Novex™, Thermo Fisher Scientific EC62252BOX) at 120-125 V for 40-90 minutes on ice (Typical native gel results can be referred to Figure S5).

Analysis of Sirt6 deacetylation of acetylated H3 and H2B nucleosomes and histones

For all the deacetylation assays with WT Sirt6 and mutants, each of the semi-synthetic free histone proteins (H3K9ac, H3K14ac, H3K18ac, H3K23ac, H3K27ac, H2BK11ac, H2BK12ac, H2BK20ac, H2B46ac, H2BK11lac, and H2BK11bhb) (final 1.0 μM) or the corresponding nucleosomes (H3K9ac, H3K14ac, H3K18ac, H3K23ac, H3K27ac, H2BK11ac, H2BK12ac, H2BK20ac, H2B46ac, H2BK11lac, and H2BK11bhb) (final 100 nM) were diluted into Sirt6 reaction buffer (50 mM HEPES at pH 7.5, 1 mM DTT, 0.2 mg/mL BSA, and 1 mM NAD).[8] The reaction solution was kept on ice until the addition of Sirt6 and then incubated at 37 ˚C. At different time points, multiple reaction samples from the same reaction tubes were taken. In a typical sample, 6.5 μL aliquots of the reaction were first taken and quenched with Dual quenching buffer (6.5 μL 4 × Laemmli sample buffer 1:1 diluted with 40 mM EDTA) to a final quenched solution with 1 × Laemmli sample buffer with 10 mM EDTA. For typical nucleosome assay, the time points contain 0, 30, 60, 90, 120 min. For typical free H3 protein assay, the time points contain 0, 5, 10, 20, 30 min, while for typical free H2B histone protein assay, the time points contain 0, 2, 4, 6, 8, 20 min. Each sample was then boiled for 3-5 min at 95 ˚C and resolved on a 4-20 % gradient SDS-PAGE gel (TGX™, Bio-Rad, 4561096) at 180 Volts for ~25 min. Gels were then transferred to nitrocellulose membrane (Transfer Stack, Invitrogen, IB301031) for western blot analysis (WB) by iBlot (Invitrogen) with P3 (20 V) for 5.0 min. Site-specific antibodies for acetylated H3 and acylated H2B, such as for anti-H3K9ac, anti-H3K14ac, anti-H3K18ac, anti-H3K23ac, anti-H3K27ac, anti-H2BK11ac (Invitrogen, #PA5-112479), anti-H2BK12ac (ActiveMotif, #39669), anti-H2BK20ac (Revmab Biosciences #31-1113-00), and anti-H2BK46ac (ActiveMotif, #39571) were used to blot the corresponding membranes. Meanwhile, anti-H3 or anti-H2B (Abcam, #ab1791, Abcam, #ab134211, or Abcam, #ab52484) was used to visualize total H3 or H2B, respectively. The affinities and specificities of the primary antibodies anti-H3K9ac, anti-H3K14ac, anti-H3K18ac, anti-H3K23ac, and anti-H3K27ac have been confirmed previously[5], while the affinities and specificities of the primary H2B antibodies were also tested and validated[2]. After secondary antibody Anti-Rabbit IgG, HRP linked antibody (Cell signaling #7074S) blotting for 1 h at room temperature, the membranes were treated with the ECL substrate reagent (Bio-Rad, #170-5061), and visualized by the G:BOX mini gel imager (Syngene). The bands on the membrane were then quantified by ImageJ (Download from imagej.nih.gov/ij/). All intensity values were divided by the intensity value at t=0 to get relative intensity, and then fit to a single-phase exponential decay curve with constrain Y0=1, Plateau=0 (GraphPad Prism 9). Each plotted point represents at least 2 replicates (Figure S5,6). The kinetic parameter V/[E] was calculated using GraphPad Prism 9. For the free histone protein assays with H3 (Figure S7) and H2B (Figure S8), a decrease in each histone loading control was observed over time (Figure 1B, Figure S7ABCE, and Figure S8ABCD), which we speculate may be due to aggregation/precipitation of these histones under the conditions of the assay. To account for this we normalized the PTM signal relative to the corresponding total histone signal at each time point. This is indicated in the Figure S7F and Figure S8E as “normalized relative intensity”. Normalization was applied before plotting and fitting to get the kinetic data for V/[E] calculation. Normalized V/[E] were calculated for histone assays (V/[E] divided by a factor

of 5) given that each nucleosome contains two H3 molecules and the final histone protein substrate (1.0 μM) is ten times more than nucleosome substrate (100 nM). The velocity data for the histone protein assays are within statistical error, and thus indistinguishable from zero rate, which we indicate as normalized V/[E] of <0.01 (Figure S7,8). The remaining nucleosome samples after assay were loaded onto a native 4-20 % TBE gels (Novex™, Thermo Fisher Scientific EC62252BOX) at 130 Volts for 110 min to compare with the samples before assay to confirm the stability of nucleosome throughout the assay (Figure S5,6). Note that in the Coomassie staining of the TBE gels the presence of extra bands is attributed to BSA multimers due to temperature[9] and buffer conditions[10].

Anti-H3K9ac antibody linearity test and antibody specificity test

A calibration curve was measured out to confirm that the substrate recognition by the anti-H3K9ac site-specific antibody was in the linear range. Different concentrations of H3K9ac nucleosome-147 were loaded followed by the primary and secondary antibody blotting as described above to get band intensity. The intensity shows good linearity with the amount of H3K9ac nucleosome-147 input (Figure S4). The antibody specificity test has been done as before.[2]

Enzyme concentration-dependent Sirt6 mutant activity assay

For all the Sirt6 mutants, an enzyme concentration-dependent assay was carried out for both acetylated H3 and H2B nucleosomes. For WT Sirt6 nucleosome deacetylation assay on H3K9ac nucleosome as an example, two different final concentrations of the Sirt6 (10 nM, 30 nM) were mixed with H3K9ac nucleosomes (Figure S3D). The rate "V" showed a linear relationship with enzyme concentration, while the V/[E] remained relatively constant (Figure S3E). Similarly, enzyme concentration-dependent assays were also carried out for all the other H3 and H2B nucleosomes. In each of these cases, the V measurements generally showed a linear relationship with enzyme concentration. For different Sirt6 mutants mean ± SD was plotted as a bar graph, in which all the V/[E] from different enzyme concentrations were taken into account for the p-value calculation (Figure S5-8).

Measuring NAD apparent Km for Sirt6 deacetylation of H3K9ac nucleosome-147

It has been reported that sirtuin family members can have different apparent affinities[11] for NAD under different acyl-Lys substrate conditions[12]. Several similar deacetylation activity assays were set up with 56.95, 227.8, 1000, or 1139 μM NAD under 10 nM WT Sirt6 and 100 nM nucleosome unchanged condition. The kinetic parameter V/[E] ± SD under each NAD concentration was calculated using GraphPad Prism 9, and then fit into Michaelis–Menten equation to calculate $K_{m(NAD)}$ and $(V/[E])_{max(NAD)}$ (Figure S9).

Measuring nucleosome apparent Km for Sirt6 deacetylation of H3K9ac nucleosome-147

A concern for measuring apparent nucleosome Km values is the uncertain nucleosome stability at low concentrations. A series of nucleosome stability tests have been carried out showing that as low as 10 nM our nucleosomes appear stable under the deacetylation activity assay conditions (data not shown). Based on this, deacetylation activity assays were performed with 10, 20, 50, 100, 200, and 400 nM nucleosomes with fixed 1000 μM NAD. In these experiments, the WT Sirt6 concentration was varied with different nucleosome concentrations so that we could accurately measure the rates of deacetylation. The kinetic parameter V/[E] ± SD under each nucleosome concentration was calculated using GraphPad Prism 9, and then fit into Michaelis–Menten equation to calculate $K_{m(Nucleosome\text{-}147)}$ and $(V/[E])_{max(Nucleosome\text{-}147)}$ (Figure S10).

Nucleosome Km measure of Sirt6 deacylation of H3K9ac nucleosome-185

Since Sirt6 has been wildly believed to prefer to bind with DNA, one possible outcome is the nucleosome with longer DNA will favor Sirt6 binding than the nucleosome with traditional 147 "601" sequence. Based on the Km measurement of H3K9ac nucleosome-147, several similar deacetylation activity assays were set up with 10, 20, 50, 100, and 200 nM H3K9ac nucleosome-185 under 1000 μM NAD unchanged condition. But the WT Sirt6 varies under different nucleosome concentration conditions to get proper and calculatable

rate constants. The kinetic parameter V/[E] ± SD under each nucleosome concentration was calculated using GraphPad Prism 9, and then fit into Michaelis–Menten equation to calculate $K_{m(Nucleosome-185)}$ and $(V/[E])_{max(Nucleosome-185)}$ (Figure S11).

NaCl effect of Sirt6 deacylation of H3K9ac nucleosome-147

Under our standard Sirt6 deacetylation activity assay conditions no NaCl was added (beyond that present in enzyme and nucleosome storage buffers). However, while testing EMSA/binding assays, we observed that at high concentrations of Sirt6 a precipitate formed, while the addition of supplemental NaCl prevented this (data not shown). This suggested NaCl concentration may affect Sirt6 stability and/or deacetylation activity, and even oligomerization state (suggested by a high molecular weight peak observed in Superdex200 purification of His-Sirt6, data not shown). We thus measured deacetylation activity with different salt concentrations including 25, 50, 100, and 250 nM NaCl using 100 nM nucleosome and 1000 μM NAD. The WT Sirt6 varies under different nucleosome concentration conditions to get proper and calculatable rate constants. The kinetic parameter V/[E] ± SD was calculated using GraphPad Prism 9 (Figure S12).

MDL-800 inhibition assay of Sirt6 with H3K9ac nucleosome-147

MDL-800 (Sigma-Aldrich #SML2529-5MG) was first prepared as stock solution in DMSO with the stock concentration of 10 mM, followed by the serial dilution from 20 μM down to 20 nM in DMSO. In each of the reaction, 2 nM WT Sirt6 was mixed with buffer containing 100, 10, 1, 0.1, 0.01 μM MDL-800 and pre-incubated at room temperature for 5 min. Buffer containing 10 % DMSO was used as a vehicle control, while buffer without DMSO was used as a positive control. After cooling on ice for 3 min, 20 nM final H3K9ac nucleosome-147 was added to initiate the deacetylation reaction. At different time points as 0, 30, 60, 120 min, multiple reaction samples from the same reaction tubes were taken, before processing as described above. The final $(V/[E] \pm SD)_{MDL\text{-}800=100,\ 10,\ 1,\ 0.1,\ 0.01\ \mu M}$ under each MDL-800 condition was calculated as described above, and then divided by the control $(V/[E] \pm SD)_{MDL\text{-}800=0,\ DMSO}$, providing the SD for each measurement (Figure S13).

Binding/activity assay with H3K9Sac nucleosome-185

To assess the binding between WT Sirt6 and H3K9Sac nucleosome-185, different nucleosome types, different WT Sirt6 concentrations, different H3K9Sac nucleosome-185 concentrations, different salt concentrations, different buffer contents have been screened (data not shown). Sirt6 binding buffer (HEPES 50 mM, NaCl 100 mM, DTT 1 mM, BSA 0.2 mg/mL, 150 μM NAD, pH=7.45) was discovered to allow both WT Sirt6 and nucleosome to be stable in solution. In a typical binding screening experiment, 400 nM H3K9Sac nucleosome-185 was mixed with 1 μM WT Sirt6 (NCP:Sirt6=1:2.5 ratio) in Sirt6 binding buffer, and was incubated on ice, room temperature, or 37 ˚C for 2h. The solution was applied to a native 4-20 % TBE gel (Figure S14A), SDS-PAGE, and WB analysis. SDS-PAGE showed no significant precipitation (data not shown), while WB analysis showed a significant decrease signal with anti-H3K9ac antibody (data not shown).

Analysis of Sirt6 deacylation with H3K9Sac nucleosome

To explain why the binding between WT Sirt6 and H3K9Sac nucleosome-185 was not as strong as expected, a typical deacetylation activity assay was set up under 10 and 30 nM WT Sirt6 condition, before processing as described above (Figure S15).

Binding/activity assay with H3K9MTU nucleosome-185

The binding assay between WT Sirt6 and H3K9MTU nucleosome-185 was done similarly to H3K9Sac. 0.2 and 1 μM WT Sirt6 were incubated with 400 nM H3K9MTU nucleosome-185 (NCP:Sir6=1:0.5 ratio and NCP:Sirt6=1:2.5 ratio) using Sirt6 binding buffer with or without 150 μM NAD. The solution was then incubated at 37 ˚C for 2h before being applied to a native 4-20 % TBE gel (Figure S14B), SDS-PAGE, and

WB analysis. SDS-PAGE showed no significant precipitation from the solution (data not shown), while WB analysis showed no significant decrease in signal by anti-H3K9ac antibody (data not shown).

Analysis of Sirt6 deacylation with H3K9MTU nucleosome

To confirm that WT Sirt6 and H3K9MTU nucleosome-185 bind without the removal of MTU, a typical deacetylation activity assay was set up under 10 and 30 nM WT Sirt6 condition, before processing as described above. Although signal is pretty weak with anti-H3K9ac antibody, there is no significant decrease after 2 h (data not shown).

Sirt6 binding H3K9MTU nucleosome-185 complex sample preparation and grid preparation

A 200 µL large-scale binding assay was set up with WT Sirt6 and H3K9MTU nucleosome-185 in Sirt6 binding buffer (400 nM NCP: 1 µM Sirt6 = 1:2.5 ratio). After incubation at 37 ˚C for 2h, the sample was centrifuged for 10 minutes at 21,300g at 4°C and loaded onto a Superose 6 Increase 3.2/300 (Cytiva) column, equilibrated in buffer (50 mM HEPES (pH 7.5) at 25°C, 1 mM TCEP, 100 mM NaCl). Absorbance was measured at 260 nm and 280 nm. Corresponding sample was collected in 50 µL fractions and analyzed by SDS-PAGE (Figure S16A-C). Fractions containing the complex were crosslinked with 0.1% (v/v) glutaraldehyde for 10 minutes on ice followed by quenching with 2.4 mM aspartate and 2 mM lysine for 10 minutes on ice. Samples were dialyzed for three hours in buffer (50 mM HEPES (pH 7.5), 1 mM TCEP 100 mM NaCl).

Quantifoil R2/1 on 200 Mesh copper grids were glow discharged for 30 s at 15 mA using a Pelco Easiglow plasma discharge system. 4 µL of dialyzed sample was applied to grids for 8 s, blotted for 5.5 s with a blot force of 8 and vitrified by plunging into liquid ethane using a Vitrobot Mark IV (FEI) at 5 °C and 100 % humidity.

Cryo-EM data collection and image processing

Cryo-EM data were collected on a ThermoFisher Titan Krios at 300 keV equipped with a Gatan K3 direct electron detector and a BioQuantum GIF energy filter. Data collection was automated using SerialEM[13] software. Two datasets were collected at a pixel size of 0.83 Å. The first data set, collected with 0° tilt and a defocus range of 0.7 to 1.7 µm, yielded 15,192 micrographs. The second data set, collected with 30° tilt and a defocus range of 0.9 to 1.9 µM, yielded 6,922 micrographs. The first dataset was collected with 44 movie frames at an exposure time of 2.802 s with an electron flux of 18.0055 e^{-} $Å^{-2}$ s^{-1} for a total exposure of 50.45 e^{-} $Å^{-2}$. The second dataset was collected with 44 movie frames at an exposure time of 2.871 s with an electron flux of 17.8487 e^{-} $Å^{-2}$ s^{-1} for a total exposure of 51.24 e^{-} $Å^{-2}$. Initial image processing was conducted in cryoSPARC (v3.2.0)[14]. Movies were aligned using cryoSPARC Live Patch Motion Correction followed by CTF estimation. The cryoSPARC Blob picker was used to pick 2,507,720 particles from the first dataset and 1,556,859 particles from the second dataset. The combined 4,064,579 particles were extracted at a box size of 350 pixels. An *ab initio* reconstruction was performed with select particles. Subsequently, three ab initio classes were placed into a heterogenous refinement job with all particles. After multiple rounds of classification and subsequent removal of junk particles, one class with a clear intact nuclesome was present. This class consisted of 595,268 particles and was further processed with global and local CTF refinements to produce a 2.9 Å reconstruction after non-uniform refinement. This was further classified using heterogenous refinement into 4 classes to enrich for Sirt6. Particles with Sirt6 bound were refined to 3.0 Å after non-uniform refinement with 251,037 particles. The resulting map had high resolution features for histones but lacked high resolution information for Sirt6 (Figure S18). Therefore, a mask encompassing Sirt6 and the extranucleosomal DNA was created in Relion, and masked classification without image alignment was performed. Upon multiple rounds of masked classifications, a resulting class with 95,205 particles was refined to 3.1 Å after non-uniform refinement in cryoSPARC (map A). To enhance local Sirt6 features and the H3 tail density, a new mask was created encompassing Sirt6 and the H3 tail was created in RELION, and masked classification without image alignment was performed. After two rounds of this, a resulting class with 81,315 particles was refined to 3.3 Å after homogenous refinement (map B). The resulting map had subsequent details required for the N-terminus of the H3 tail. Maps were

post-processed with Noise2map (map A) and cryoSPARC (map B) and local resolution was determined using cryoSPARC. Angular distribution plots were generated using the available software in WARP (Table S2).[15]

Model building and figure preparation

Initial structures of the nucleosome (PDB 3LZ0)[16], H3 tail (PDB 5Y2F), Sirt6 (PDB 5Y2F)[17], and Sirt6 N-terminal residues 2-16 (AlphaFold2)[18] were rigid body docked into the electron density (map A and B). Residues 17 to 83 of Sirt6 are partially less well-resolved and were rigid body docked according to the available crystal structures (PDB 5Y2F). We observe additional density for the acidic patch binding region of Sirt6 on the opposite site of the nucleosomal disk as well. Additional H3 tail residues were manually built with Coot[19]. Extranucleosomal DNA on the Sirt6 binding side was built in ChimeraX[20] and further locally adjusted in Coot. DNA on the other side of the nucleosome (opposite of Sirt6 binding side) was only partially visible in the region from ~SHL 4 to SHL 7. However, the DNA is visible upon low pass filtering, therefore the DNA from PDB 3LZ0 was maintained in the final model. The ADP-ribose analog was built in PyMol with restraints obtained from ELBOW in PHENIX[21] and docked into corresponding density based on NAD (PDB 5Y2F). The resulting structure was locally real-space refined using Coot. Final models were real space refined in PHENIX using map A, secondary restraints from PDB 5Y2F (Sirt6) and 3LZ0 (nucleosome) with global minimization, local rotamer fitting, adp refinement and restraints generated from the ELBOW job (Table S3).

All figures with cryo-EM maps and structural models were prepared using ChimeraX. Graphs were plotted in GraphPad Prism, and final figures were assembled in Adobe Illustrator.

LC-MS analysis of Sirt6 binding/reacting with H3K9MTU nucleosome-185

The purest fractions from the micro gel filtration were combined and repurified by HPLC using a TSKgel DEAE-5PW ion exchange column (TOSOH Bioscience, #83W-00096C). Nucleosomes were separated by the apparent number of bound Sirt6 molecules (2, 1 or 0) using buffers A TES150 (10 mM Tris pH 7.5, 150 mM KCl, 0.5 mM EDTA) and B TES600 (10 mM Tris pH 7.5, 600 mM KCl, 0.5 mM EDTA) with the following gradient: 22% B for 3 minutes, 22-54% B for 1 minute, 54-75% B for 21 minutes, 75-100% B for 1 minute. Fractions containing nucleosome modified with two Sirt6 were immediately diluted with one volume of TCS Buffer (20 mM Tris at pH 7.5 and 1 mM DTT), then concentrated (30 kDa MWCO Amicon Ultra 4 mL, EMD Millipore) at 4 ˚C. Concentration was assessed using the absorbance at 260 nm, and samples were diluted to a DNA concentration of 10 ng/μL in 6 M guanidine, 1.6 M sodium chloride. This sample was analyzed by RP-HPLC (Vanquish HPLC, Thermo Scientific; MAbPac 2.1 x 100 mm, 4 μm Ph, Thermo Scientific) coupled to ESI-MS (Q Exactive, Thermo Scientific). Using water with 0.1% formic acid and acetonitrile with 0.1% formic acid as mobile phases A and B respectively, sample (3 uL) was separated over a 17 minute 25-40% B gradient following an initial 2 minute wash at 0% B. Mass spectra were deconvoluted using UniDec.[1] (Figure S20)

Sirt6(1-355) M1C $[M]^+$: calculated as m/z 39090.82 , observed as m/z 39087.1;
H4 $[M]^+$: calculated as m/z 11236.15, observed as m/z 11235.4;
H2B $[M]^+$: calculated as m/z 13493.68, observed as m/z: 13493.1;
H2A $[M]^+$: calculated as m/z 13950.20, observed as m/z 13949.4;
WT-H3: $[M]^+$ calculated as m/z 15238.8, observed as m/z 15238.0;
H3K9MTU: $[M]^+$ calculated as m/z 15311.7, observed as m/z 15311.2;
H3K9 Nε-1,3-oxathiolan-2-ylidene amine intermediate analog $[M]^+$: calculated as m/z 15821.97, observed as m/z 15821.4.

Analysis of Sirt6 mutant deacetylation with H3K9ac nucleosome-147

All six Sirt6 mutants were expressed and purified as described above. Densitometry based on Coomassie staining with BSA as standard was used to measure each concentration and to confirm the purity (data not shown). Deacetylation activity assays were set up (as described above) with 100 nM H3K9ac nucleosome-147 and 1000 μM NAD with each Sirt6 mutant, before processing as described above (Figure S21,22).

EMSA of Sirt6 mutants with H3K9ac nucleosome-185

To assess WT Sirt6 and Sirt6 mutants to nucleosome, EMSA assays with WT Sirt6 and each Sirt6 mutant were performed. The Sirt6 proteins were diluted to a working stock solution of 9.6 μM, followed by serial dilution to 4800, 2400, 1200, 600, 300, 150, 75, 0 nM in each tube. A final concentration of 20 nM solution of H3K9ac nucleosome-185 in Sirt6 binding buffer without 150 μM NAD was added and mixed to each tube to reach final Sirt6 concentration as 960, 480, 240, 120, 60, 30, 15, 0 nM. The solution was incubated for 30 min on ice, followed by being applied to a native 4-20 % TBE gel. The whole assay has been conducted for at least 2 times (Figure S23).

Supplemental References

(1) Marty, M. T.; Baldwin, A. J.; Marklund, E. G.; Hochberg, G. K. A.; Benesch, J. L. P.; Robinson, C. V. Bayesian deconvolution of mass and ion mobility spectra: From binary interactions to polydisperse ensembles. *Anal Chem*. **2015**, *87* (8), 4370–4376.

(2) Wang, Z. A.; Whedon, S. D.; Wu, M.; *et al.* Histone H2B Deacylation Selectivity: Exploring Chromatin's Dark Matter with an Engineered Sortase. *J Am Chem Soc*. **2022**, *144* (8), 3360−3364.

(3) Luger, K.; Rechsteiner, T. J.; Richmond, T. J. Preparation of Nucleosome Core Particle from Recombinant Histones. *Methods Enzymol*. **1999**, *304* (1997), 3–19.

(4) Gatchalian, J.; Wang, X.; Ikebe, J.; *et al.* Accessibility of the histone H3 tail in the nucleosome for binding of paired readers. *Nat Commun*. **2017**, *8* (1), .

(5) Wang, Z. A.; Millard, C. J.; Lin, C.-L.; *et al.* Diverse nucleosome site-selectivity among histone deacetylase complexes. *eLife*. **2020**, *9*, e57663.

(6) Wu, M.; Hayward, D.; Kalin, J. H.; Song, Y.; Schwabe, J. W.; Cole, P. A. Lysine-14 acetylation of histone H3 in chromatin confers resistance to the deacetylase and demethylase activities of an epigenetic silencing complex. *eLife*. **2018**, *7*, e37231.

(7) Dyer, P. N.; Raji, E. S.; White, C. L.; *et al.* Reconstitution of Nucleosome Core Particles from Recombinant Histones and DNA. *Methods Enzymol*. **2004**, *375*, 23–44.

(8) Watson, P. J.; Millard, C. J.; Riley, A. M.; *et al.* Insights into the activation mechanism of class i HDAC complexes by inositol phosphates. *Nat Commun*. **2016**, *7* (11262), 1–13.

(9) Madeira, P. P.; Rocha, I. L. D.; Rosa, M. E.; Freire, M. G.; Coutinho, J. A. P. On the aggregation of bovine serum albumin. *J Mol Liq*. **2022**, *349*, 118183.

(10) Holm, N. K.; Jespersen, S. K.; Thomassen, L. V.; *et al.* Aggregation and fibrillation of bovine serum albumin. *Biochim Biophys Acta - Proteins Proteomics*. **2007**, *1774* (9), 1128–1138.

(11) Madsen, A. S.; Andersen, C.; Daoud, M.; *et al.* Investigating the Sensitivity of NAD+-dependent Sirtuin Deacylation Activities to NADH. *J Biol Chem*. **2016**, *291* (13), 7128–7141.

(12) Feldman, J. L.; Dittenhafer-Reed, K. E.; Kudo, N.; *et al.* Kinetic and structural basis for Acyl-group selectivity and NAD+ dependence in sirtuin-catalyzed deacylation. *Biochemistry*. **2015**, *54* (19), 3037–3050.

(13) Mastronarde, D. N. Automated electron microscope tomography using robust prediction of specimen movements. *J Struct Biol*. **2005**, *152* (1), 36–51.

(14) Punjani, A.; Rubinstein, J. L.; Fleet, D. J.; Brubaker, M. A. CryoSPARC: Algorithms for rapid unsupervised cryo-EM structure determination. *Nat Methods*. **2017**, *14* (3), 290–296.

(15) Tegunov, D.; Cramer, P. Real-time cryo-electron microscopy data preprocessing with Warp. *Nat Methods*. **2019**, *16* (11), 1146–1152.

(16) Vasudevan, D.; Chua, E. Y. D.; Davey, C. A. Crystal Structures of Nucleosome Core Particles Containing the “601” Strong Positioning Sequence. *J Mol Biol*. **2010**, *403* (1), 1–10.

(17) Huang, Z.; Zhao, J.; Deng, W.; *et al.* Identification of a cellularly active SIRT6 allosteric activator. *Nat Chem Biol*. **2018**, *14* (12), 1118–1126.

(18) Jumper, J.; Evans, R.; Pritzel, A.; *et al.* Highly accurate protein structure prediction with AlphaFold. *Nature*. **2021**, *596* (7873), 583–589.

(19) Emsley, P.; Cowtan, K. Coot: Model-building tools for molecular graphics. *Acta Crystallogr Sect D Biol Crystallogr*. **2004**, *60* (12 I), 2126–2132.

(20) Pettersen, E. F.; Goddard, T. D.; Huang, C. C.; *et al.* UCSF ChimeraX: Structure visualization for researchers, educators, and developers. *Protein Sci*. **2021**, *30* (1), 70–82.

(21) Adams, P. D.; Grosse-Kunstleve, R. W.; Hung, L. W.; *et al.* PHENIX: Building new software for automated crystallographic structure determination. *Acta Crystallogr Sect D Biol Crystallogr*. **2002**, *58* (11), 1948–1954.

Figure SI 1-23

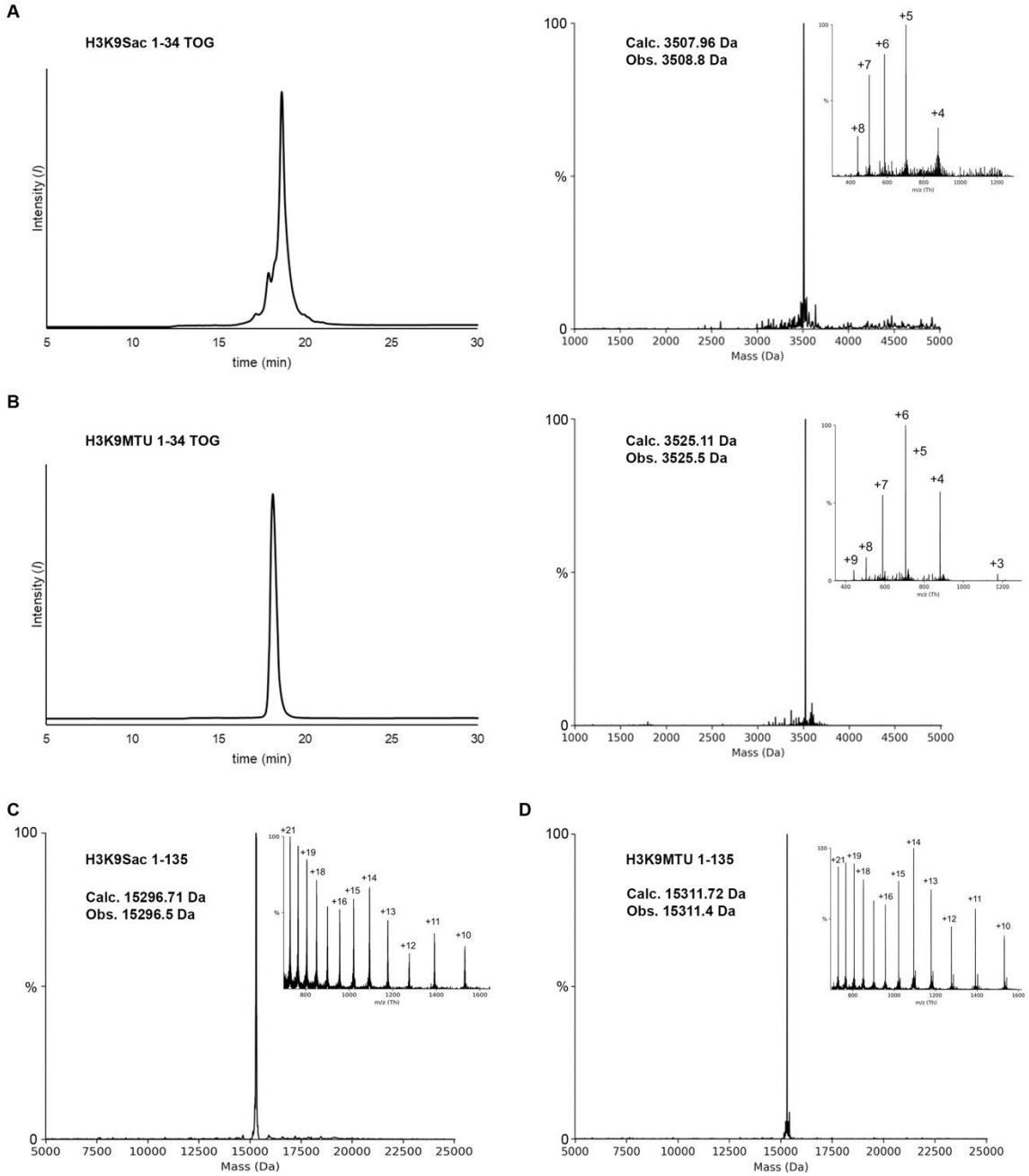

Figure S1. H3 peptides and semisynthetic H3 protein characterization. (A) Analytical RP-HPLC chromatogram (C18, 7-30% B, 30 min), intact peptide ESI-MS (inset), and deconvoluted peptide ESI-MS for H3K9Sac 1-34 TOG (Calculated exact mass for $C_{146}H_{262}N_{54}O_{44}S$ $[M]^+$: 3507.96 Da; Observed: 3508.8 Da). (B) Analytical RP-HPLC chromatogram (C18, 7-30% B, 30 min), intact peptide ESI-MS (inset), and deconvoluted peptide ESI-MS for H3K9MTU 1-34 TOG (Calculated exact mass for $C_{146}H_{263}N_{55}O_{44}S$ $[M]^+$: 3525.11 Da; Observed: 3525.5 Da). (C) Intact protein ESI-MS (inset) and deconvoluted protein ESI-MS for H3K9Sac 1-135 protein (Calculated average mass for $C_{672}H_{1133}N_{215}O_{186}S_3$ $[M]^+$: 15296.71 Da; Observed: 15296.5 Da). (D) Intact protein ESI-MS (inset) and deconvoluted protein ESI-MS for H3K9MTU 1-135 protein (Calculated average mass for $C_{672}H_{1134}N_{216}O_{186}S_3$ $[M]^+$: 15311.72 Da; Observed: 15311.4 Da).

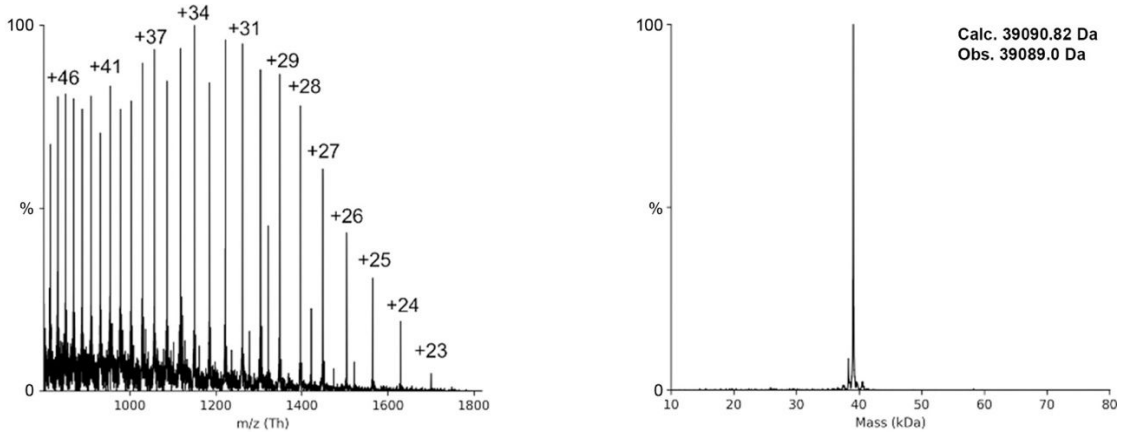

Figure S2. ESI for WT Sirt6. Intact protein ESI-MS and deconvoluted protein ESI-MS for WT Sirt6. Calculated average mass for $C_{1718}H_{2770}N_{514}O_{503}S_{13}$ [M]+: 39090.82 Da; Observed: 39089.0 Da.

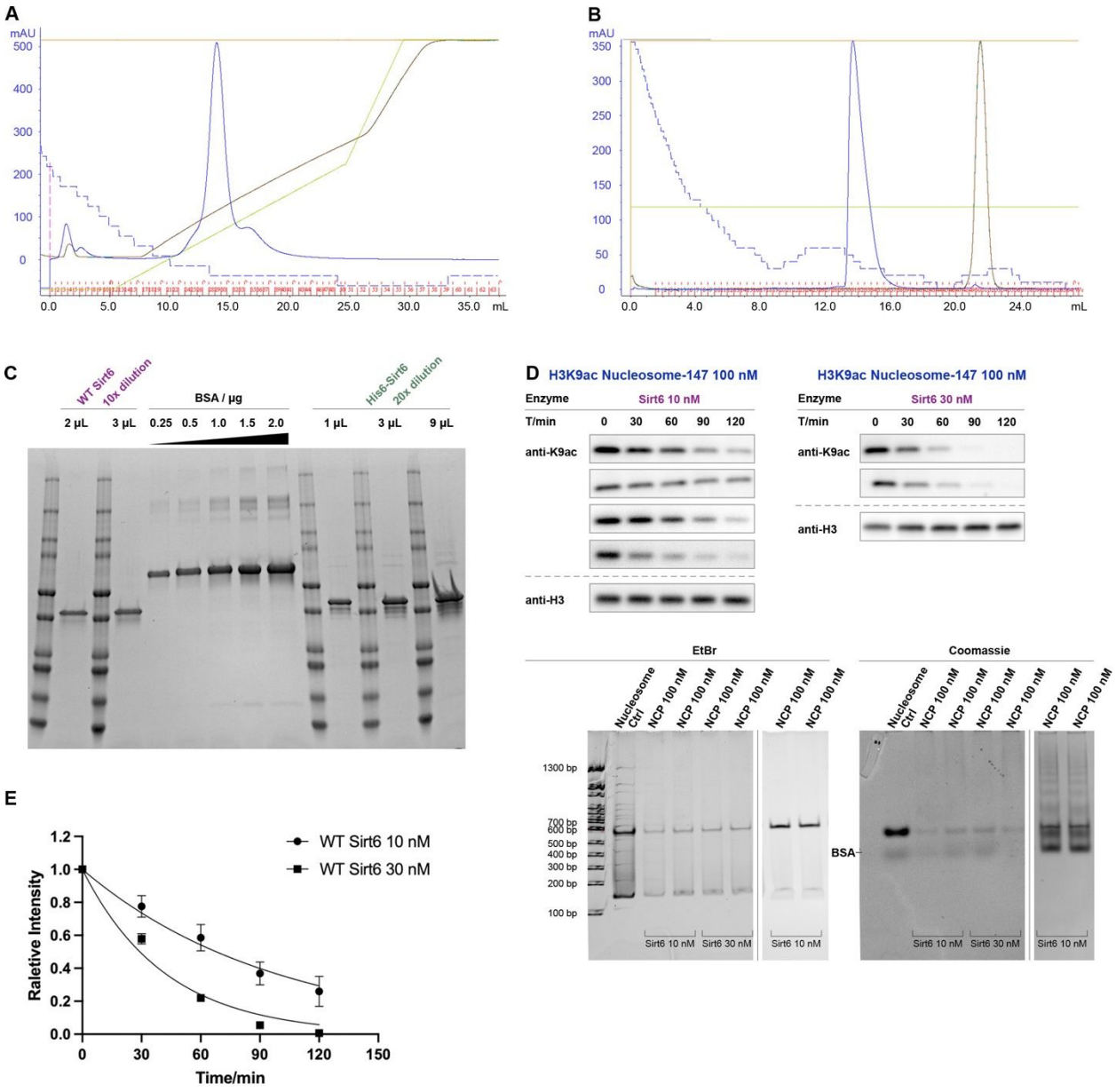

Figure S3. WT Sirt6 purification and activity measurement. (A) Heparin column FPLC chromatography for WT Sirt6 purification. (B) Superdex200 column FPLC chromatography for WT Sirt6 purification. (C) SDS-PAGE and Coomassie staining of final WT Sirt6 before and after TEV cleavage. (D) Western blot of WT Sirt6 (10 nM, 30 nM) deacetylation assay on H3K9ac nucleosome. (E) Curve fitting for nucleosome kinetics with 10, 30 nM WT Sirt6.

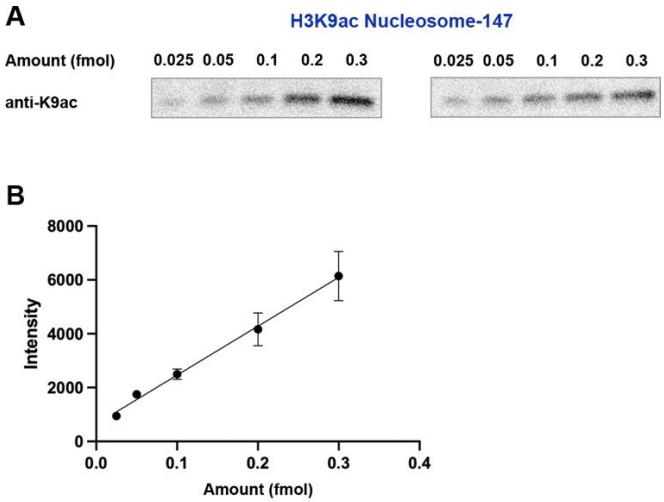

Figure S4. Anti-H3K9ac antibody linearity test. A series of 0.025, 0.05, 0.1, 0.2, and 0.3 fmol of H3K9ac nucleosome-147 were resolved by SDS-PAGE, transferred, blocked and blotted with primary anti-H3K9ac antibody, followed by HRP secondary antibody, and ECL to get band intensity. The intensity was then plotted with H3K9ac nucleosome-147 amount to determine the linear detection range.

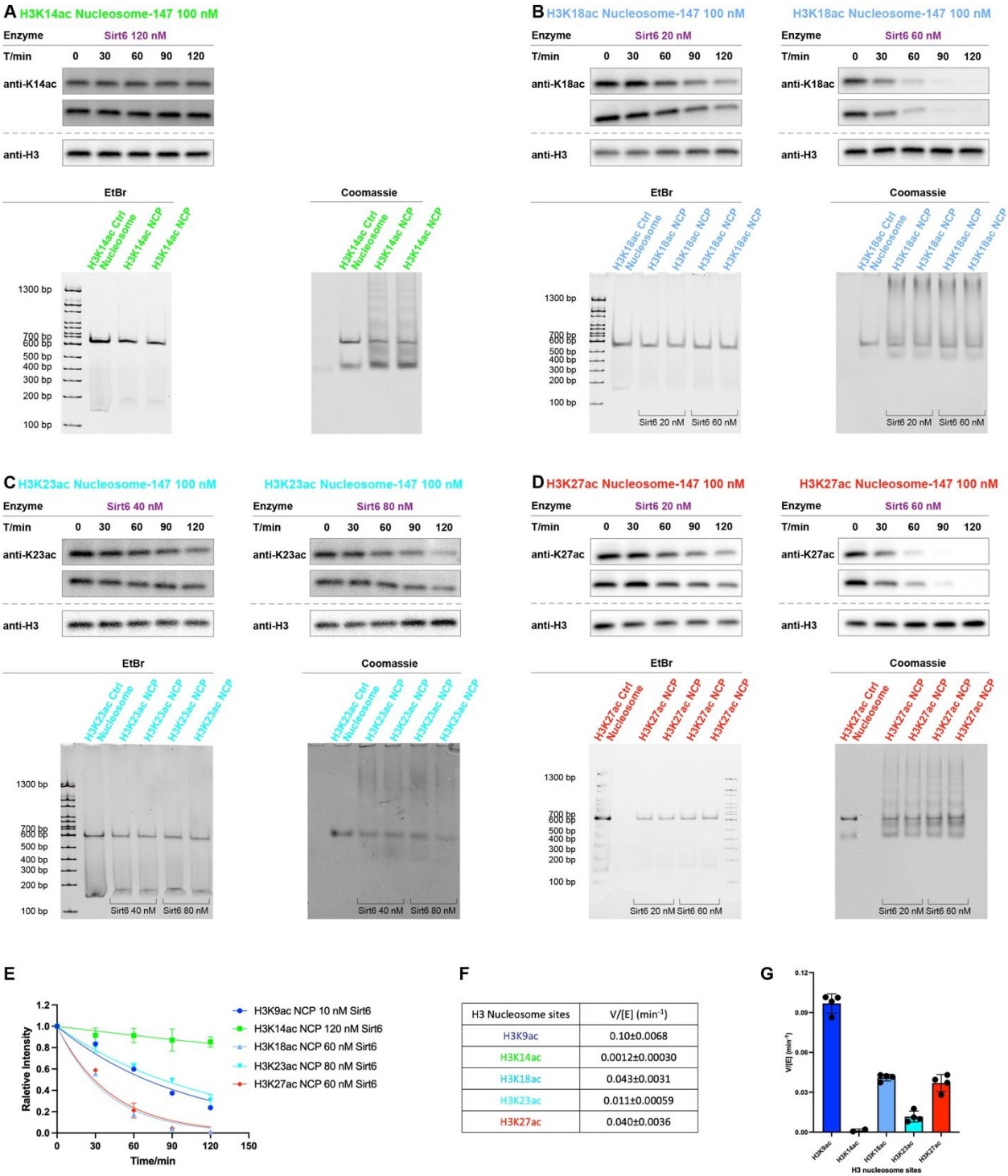

Figure S5. WT Sirt6 deacetylation on different H3 nucleosome sites. Western blot of WT Sirt6 (1 or 2 different concentrations) deacetylation assay on (A) H3K14ac, (B) H3K18ac, (C) H3K23ac, (D) H3K27ac; (E) Curve fitting for H3 nucleosome kinetics with different concentration of WT Sirt6. (F) Table for H3 nucleosome kinetics. (G) Bar graph for H3 nucleosome kinetics.

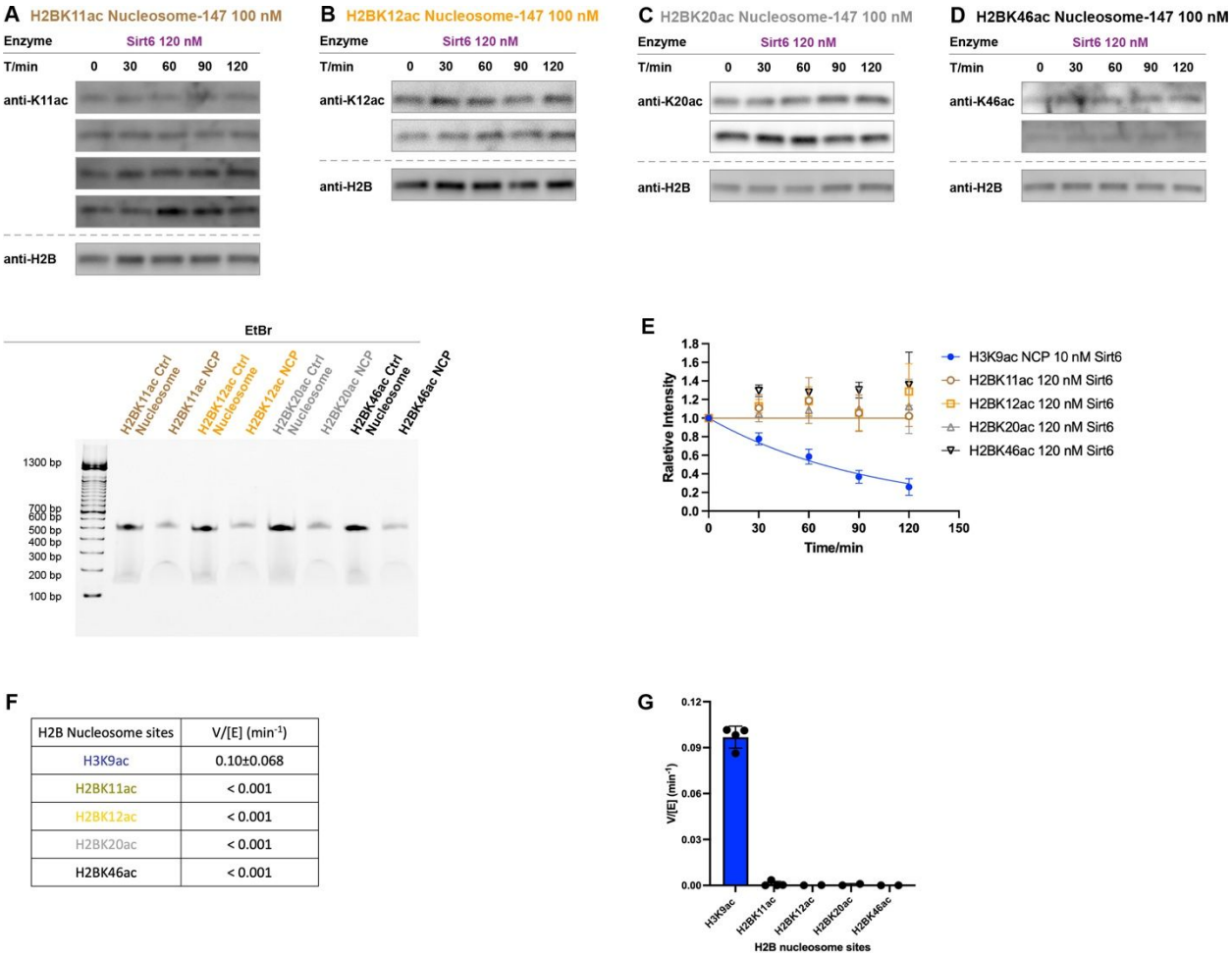

H2B Nucleosome sites	V/[E] (min^{-1})
H3K9ac	0.10±0.068
H2BK11ac	< 0.001
H2BK12ac	< 0.001
H2BK20ac	< 0.001
H2BK46ac	< 0.001

Figure S6. WT Sirt6 deacetylation on different H2B nucleosome sites. Western blot of WT Sirt6 (120 nM) deacetylation assay on (A) H2BK11ac, (B) H2BK12ac, (C) H2BK20ac, (D) H2BK46ac; (E) Curve fitting for H2B nucleosome kinetics with different concentration of WT Sirt6. (F) Table for H2B nucleosome kinetics. (G) Bar graph for H2B nucleosome kinetics.

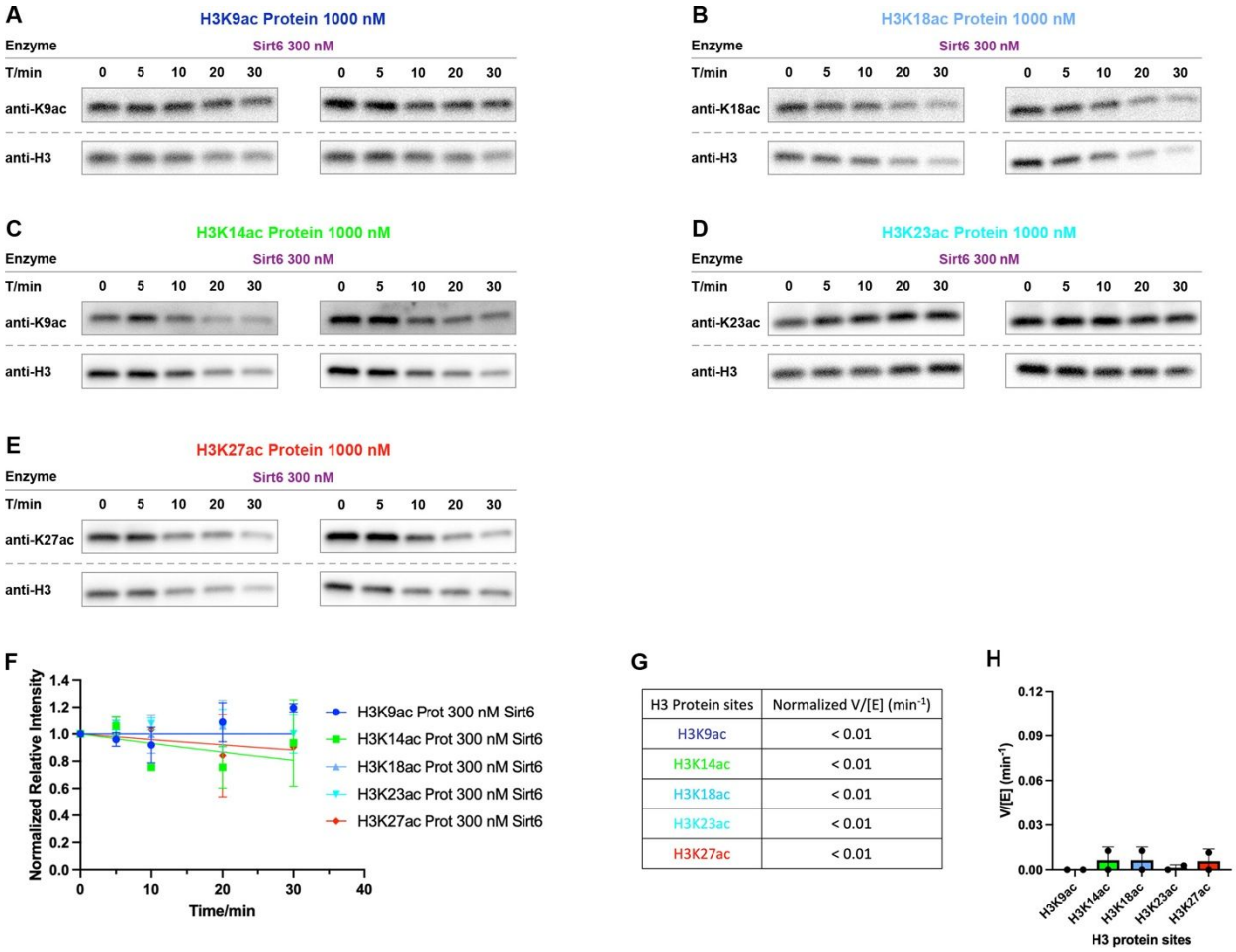

G

H3 Protein sites	Normalized V/[E] (min^{-1})
H3K9ac	< 0.01
H3K14ac	< 0.01
H3K18ac	< 0.01
H3K23ac	< 0.01
H3K27ac	< 0.01

Figure S7. WT Sirt6 deacetylation on different free H3 protein sites. Western blot of WT Sirt6 (300 nM) deacetylation assay on (A) H3K9ac, (B) H3K14ac, (C) H3K18ac, (D) H3K23ac, (E) H3K27ac. (F) Curve fitting for free H3 protein kinetics with different concentration of WT Sirt6. To account for the decrease of anti-H3 signal, we normalized the PTM signal relative to the corresponding total histone signal at each time point. (G) Table for free H3 protein kinetic parameters. (H) Bar graph for free H3 protein kinetic parameters.

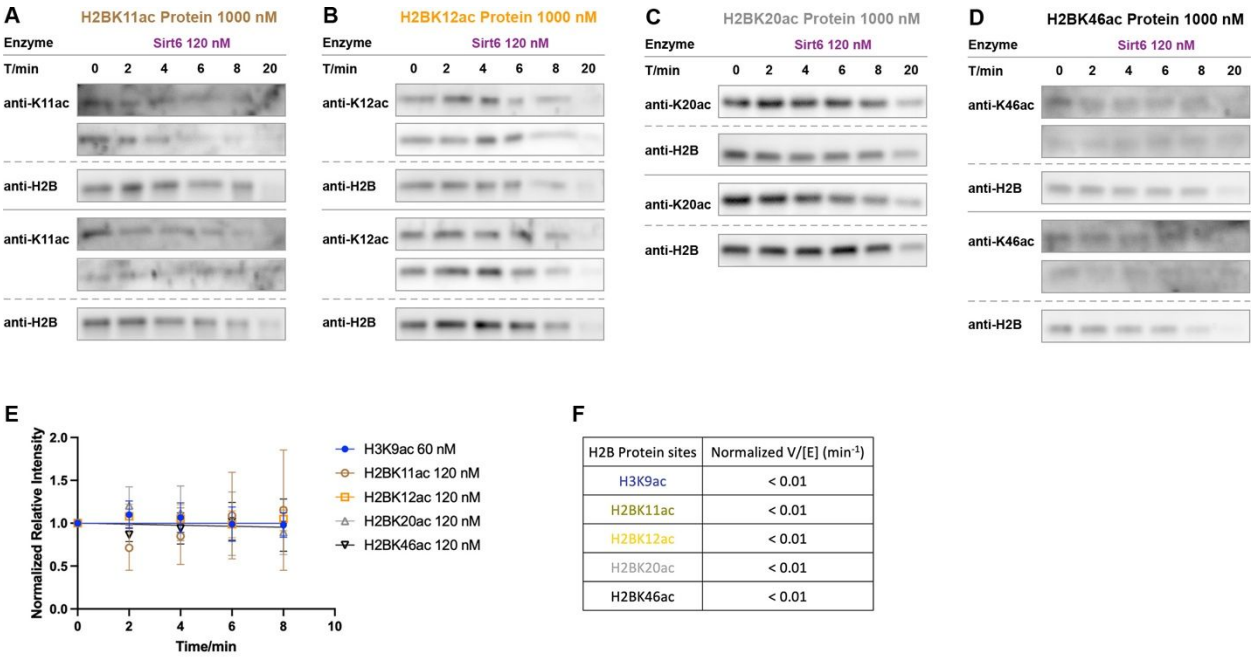

E

F

H2B Protein sites	Normalized V/[E] (min^{-1})
H3K9ac	< 0.01
H2BK11ac	< 0.01
H2BK12ac	< 0.01
H2BK20ac	< 0.01
H2BK46ac	< 0.01

Figure S8. WT Sirt6 deacetylation on different free H2B protein sites. Western blot of WT Sirt6 (300 nM) deacetylation assay on (A) H2BK11ac, (B) H2BK12ac, (C) H2BK20ac, (D) H2BK46ac; (E) Curve fitting for free H2B histone kinetics with different concentration of WT Sirt6. To account for the decrease of anti-H2B signal, we normalized the PTM signal relative to the corresponding total histone signal at each time point. (F) Table for free H2B protein kinetic parameters.

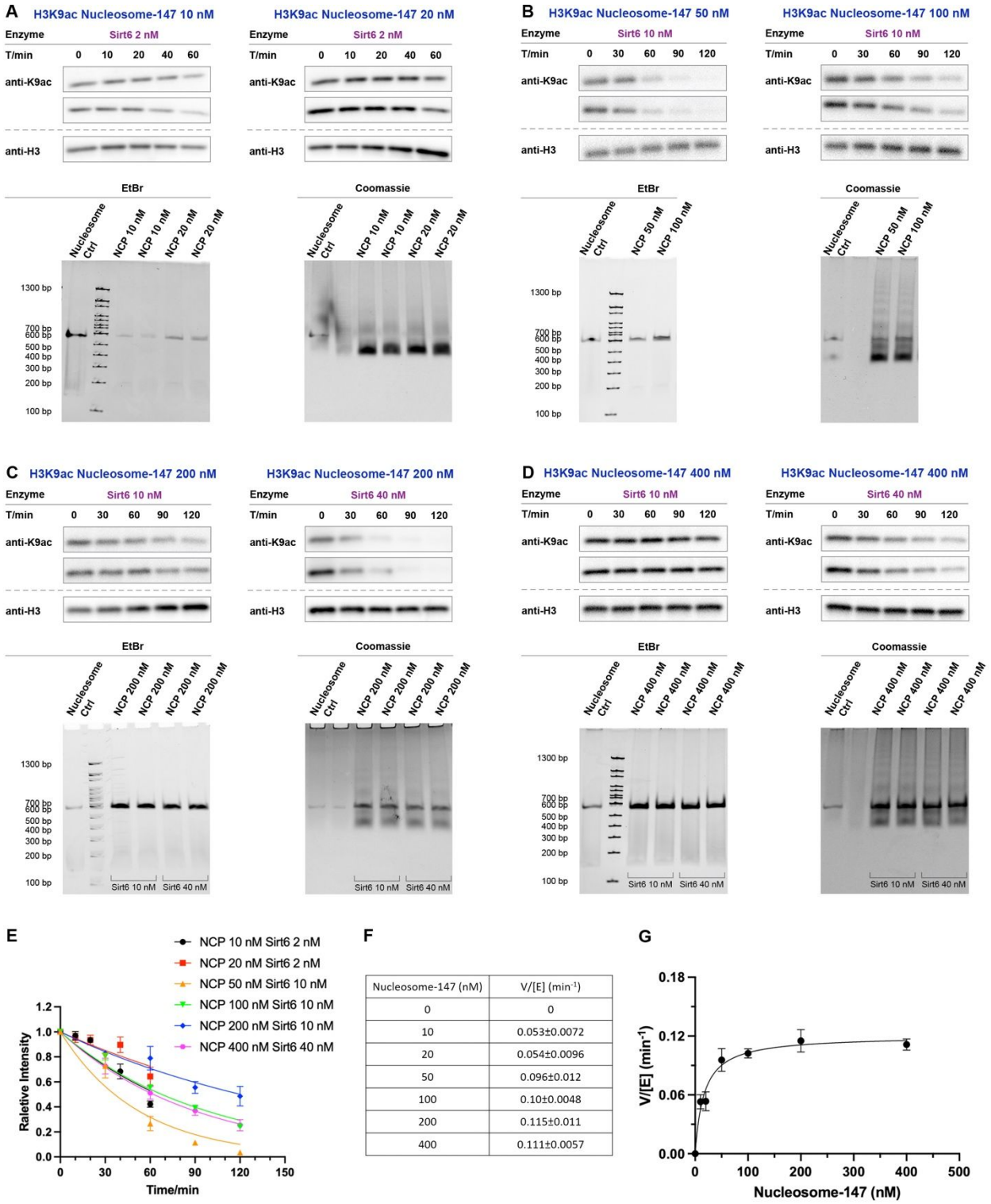

Figure S9. Km of WT Sirt6 for H3K9ac nucleosome-147. Western blot of WT Sirt6 (1 or 2 different concentrations) deacetylation assay on H3K9ac nucleosome-147 with nucleosome final concentration as (A) 10 & 20 nM, (B) 50 & 100 nM, (C) 200 nM, (D) 400 nM. (E) Curve fitting for H3K9ac nucleosome kinetics with different nucleosome final concentration. (F) Table for H3K9ac nucleosome kinetics with different nucleosome final concentration. (F) Michaelis–Menten curve fitting for V/[E] at different nucleosome concentrations.

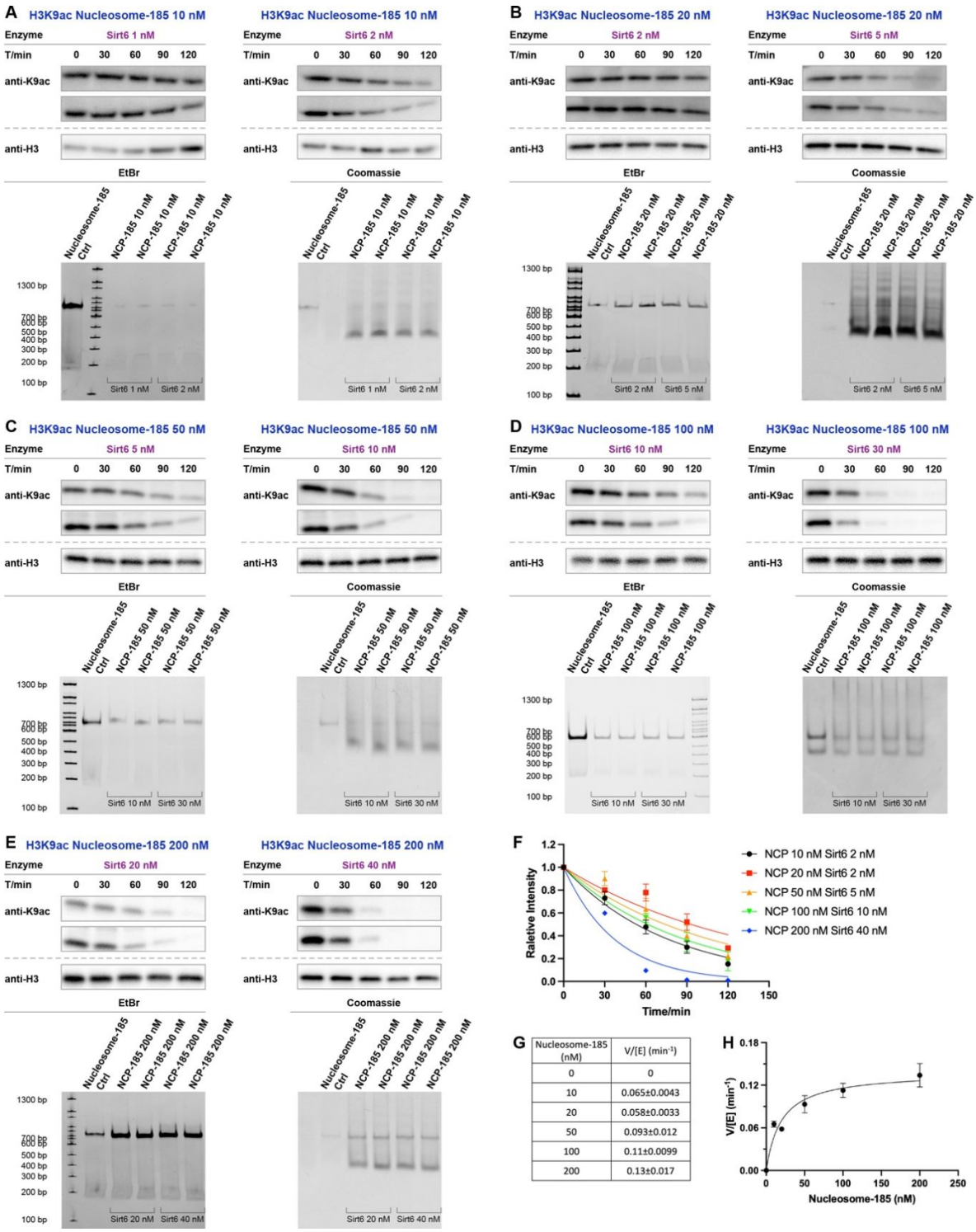

Nucleosome-185 (nM)	V/[E] (min^{-1})
0	0
10	0.065±0.0043
20	0.058±0.0033
50	0.093±0.012
100	0.11±0.0099
200	0.13±0.017

Figure S10. Km of WT Sirt6 for H3K9ac nucleosome-185. Western blot of WT Sirt6 (1 or 2 different concentrations) deacetylation assay on H3K9ac nucleosome-185 with nucleosome final concentration as (A) 10 nM, (B) 20 nM, (C) 50 nM, (D) 100 nM. (E) 200 nM. (F) Curve fitting for H3K9ac nucleosome kinetics with different nucleosome final concentration. (G) Table for H3K9ac nucleosome kinetics with different nucleosome final concentration. (H) Michaelis–Menten curve fitting for V/[E] at different nucleosome concentrations.

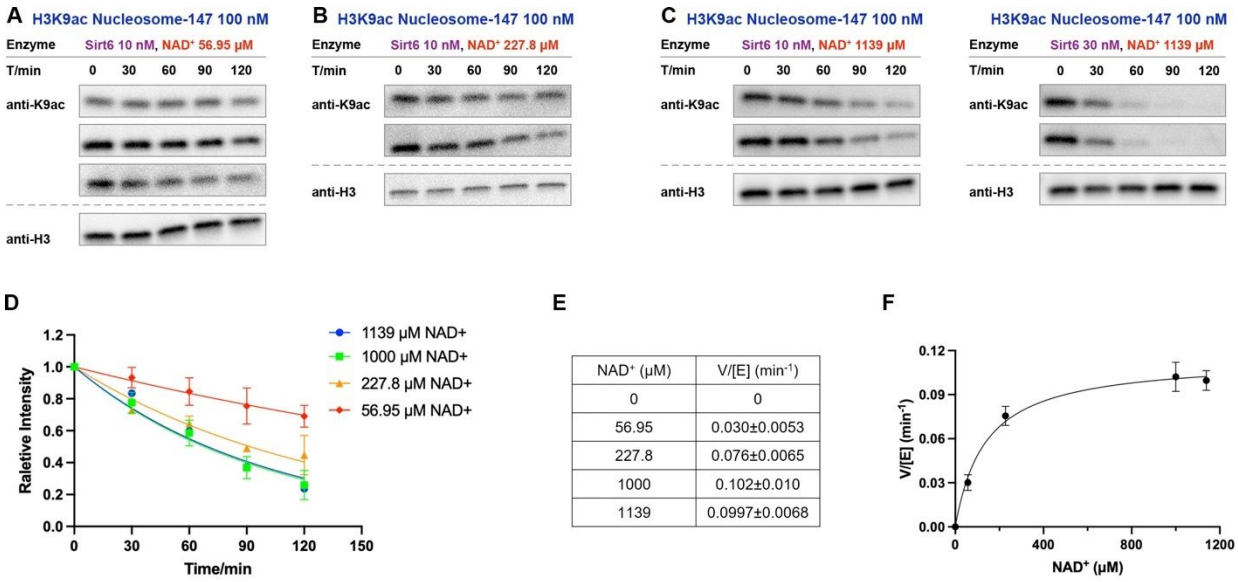

NAD⁺ (μM)	V/[E] (min⁻¹)
0	0
56.95	0.030±0.0053
227.8	0.076±0.0065
1000	0.102±0.010
1139	0.0997±0.0068

Figure S11. Km of WT Sirt6 for NAD. Western blot of WT Sirt6 (10 nM and 30 nM) deacetylation assay on H3K9ac nucleosome-147 with (A) 56.95, (B) 227.8, (C) 1139 μM NAD. (D) Curve fitting for H3K9ac nucleosome kinetics with different concentration of NAD. (E) Table for H3K9ac nucleosome kinetic parameters with different concentration of NAD. (F) Michaelis–Menten curve fitting for V/[E] with different concentration of NAD.

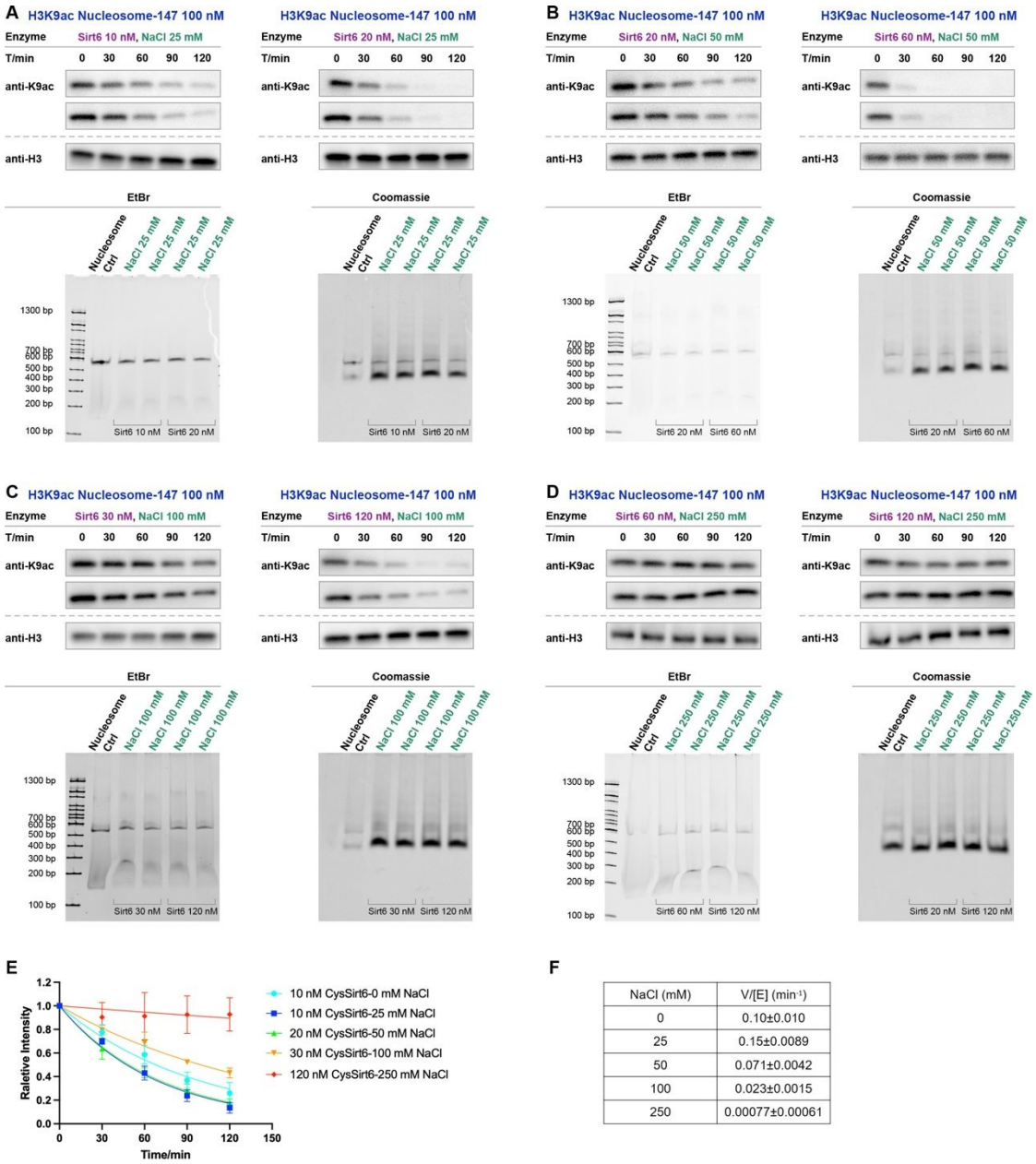

NaCl (mM)	V/[E] (min^{-1})
0	0.10±0.010
25	0.15±0.0089
50	0.071±0.0042
100	0.023±0.0015
250	0.00077±0.00061

Figure S12. Effect of NaCl on WT Sirt6 activity toward H3K9ac nucleosome-147. Western blot of WT Sirt6 (1 or 2 different concentrations) deacetylation assay on H3K9ac nucleosome-147 with different buffer NaCl concentration as (A) 25 nM, (B) 50 nM, (C) 100 nM, (D) 250 nM. (E) Curve fitting for H3K9ac nucleosome kinetics with different buffer NaCl concentration. (F) Table for H3K9ac nucleosome kinetics with different buffer NaCl concentration.

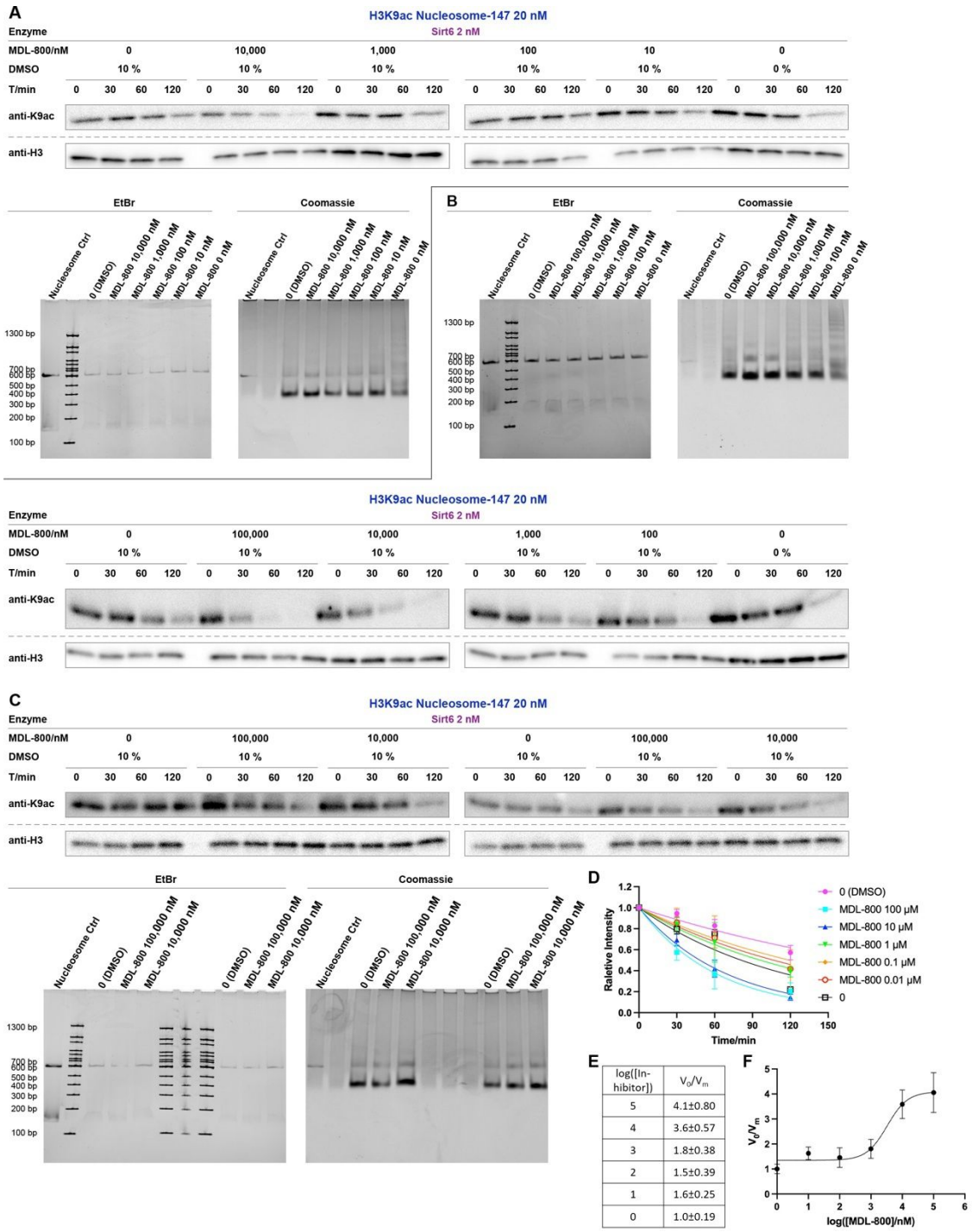

log([Inhibitor])	V_0/V_m
5	4.1±0.80
4	3.6±0.57
3	1.8±0.38
2	1.5±0.39
1	1.6±0.25
0	1.0±0.19

Figure S13. MDL-800 activation assay on H3K9ac nucleosome-147. Western blot of 2 nM WT Sirt6 deacetylation assay on 20 nM H3K9ac nucleosome-147 with (A-C) different concentration of MDL-800 in 10 % DMSO, DMSO vehicle alone, or no DMSO. (D) Curve fitting for H3K9ac nucleosome kinetics with different MDL-800 concentration. (E) Table of H3K9ac nucleosome kinetic parameters at different MDL-800 concentrations. (F) Curve fitting of "log(activator) vs. response -- Variable slope (four parameters)" with logEC50(nM) = 3.5±0.25 (EC50 = ~3.3±2.0 μM), Hill slope = 1.3.

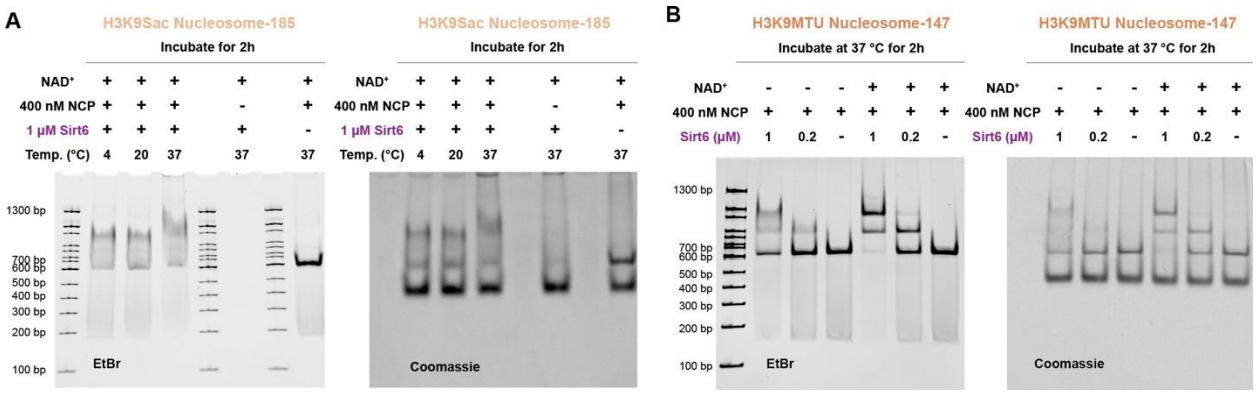

Figure S14. EMSA for H3K9Sac and H3K9MTU nucleosome-185. (A) EMSA of WT Sirt6 binding with H3K9Sac nucleosome-185 at different temperatures. (B) EMSA of WT Sirt6 binding with H3K9MTU nucleosome-185 with or without NAD.

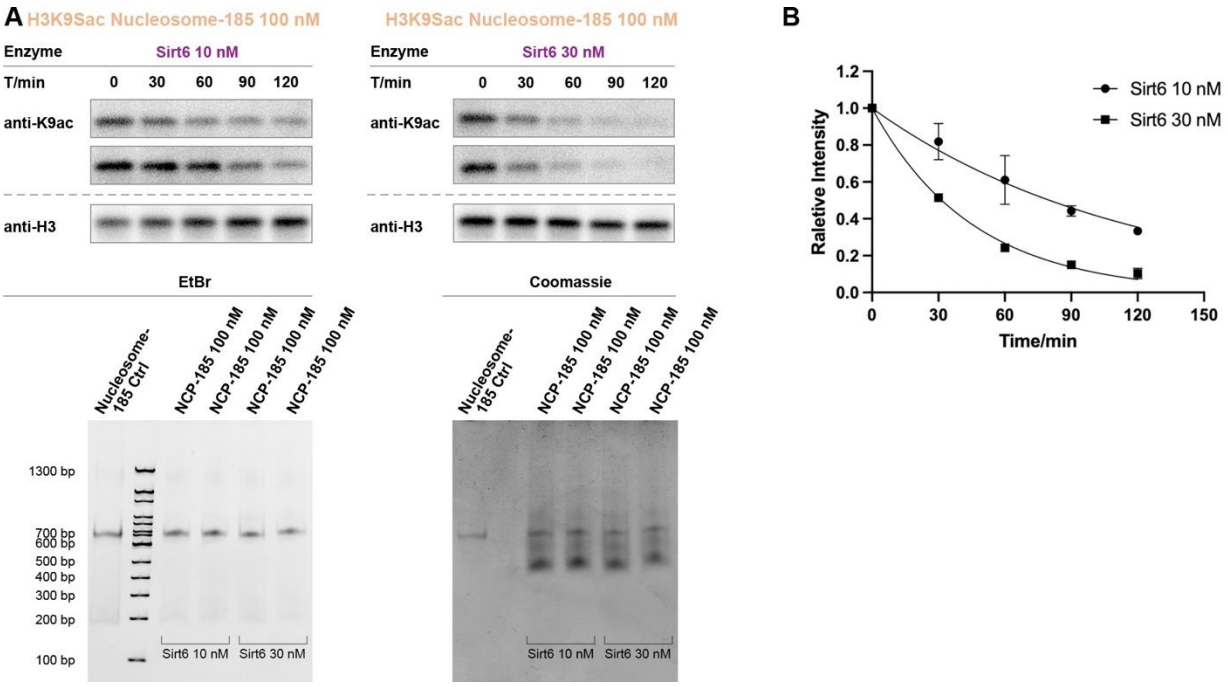

Figure S15. Western blot and curve fitting for deacylation by the H3K9Sac nucleosome-185. (A) Western blot of WT Sirt6 (10 or 30 nM) deacetylation assay on H3K9Sac nucleosome-185. (B) Curve fitting for H3K9Sac nucleosome kinetics at different concentrations of WT Sirt6.

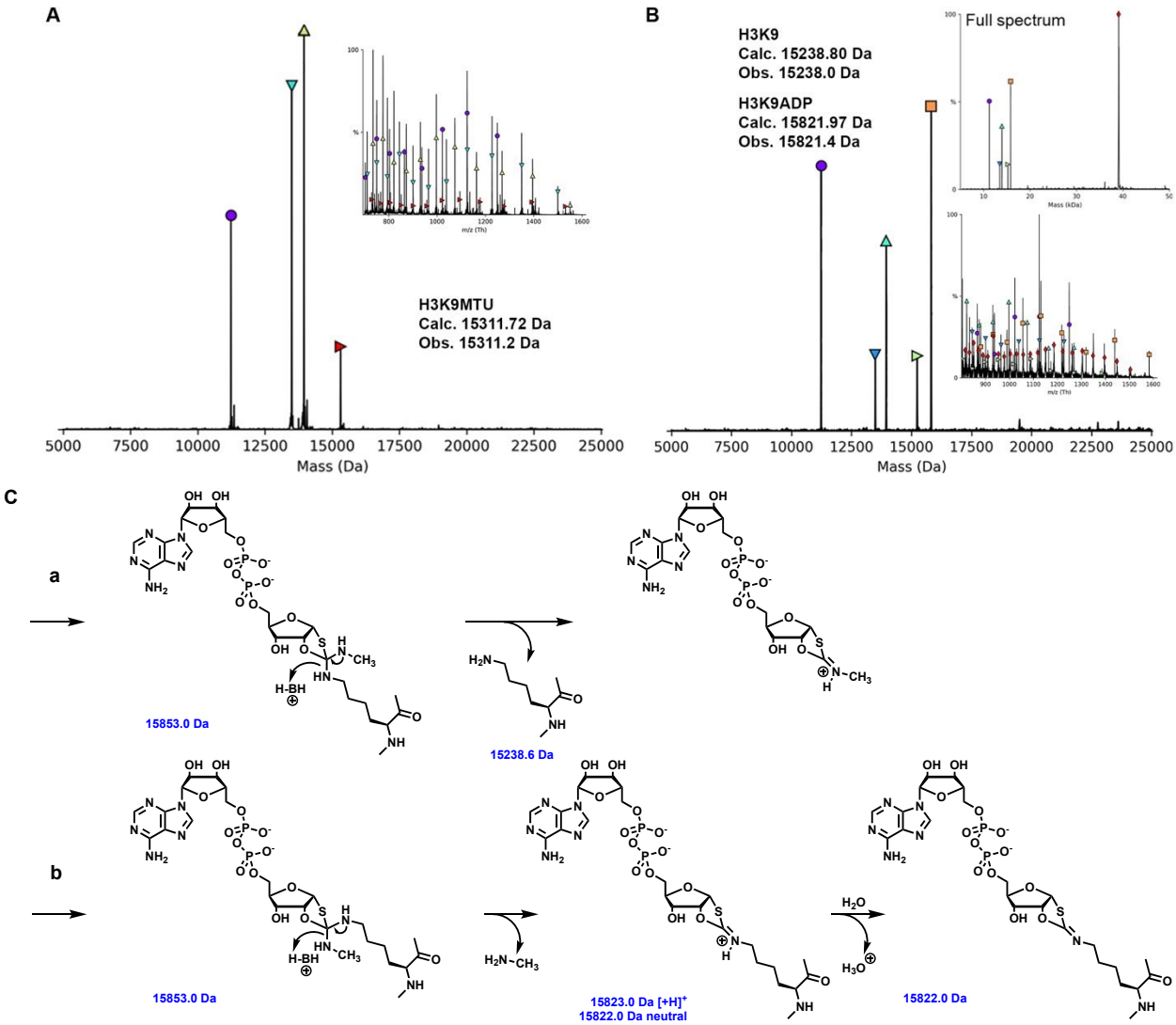

Figure S16. ESI and mechanism of WT Sirt6 binding with H3K9MTU nucleosome-185. (A) Intact ESI-MS (inset) and deconvoluted mass spectrum of H3K9MTU nucleosome-185 before binding to WT Sirt6; H4 (purple circle), H2B (downward-pointed cyan triangle), H2A (upward-pointed yellow-green triangle) and H3K9MTU (rightward-pointed red triangle). (B) Intact ESI-MS (lower inset) and deconvoluted mass spectrum of H3K9MTU nucleosome-185 after binding to WT Sirt6 (upper inset) ; H4 (purple circle), H2B (downward-pointed blue triangle), H2A (upward-pointed cyan triangle), unmodified H3 (rightward-pointed yellow-green triangle), H3K9 Nε-1,3-oxathiolan-2-ylidene amine intermediate (orange square), and Sirt6 (red diamond). (C) Scheme for catalytic activity of WT Sirt6 on H3K9MTU nucleosome-185 with intermediate analog and product masses listed in blue. Pathway a to remove the thiourea group to generate unmodified H3; Pathway b to generate the intermediate analog.

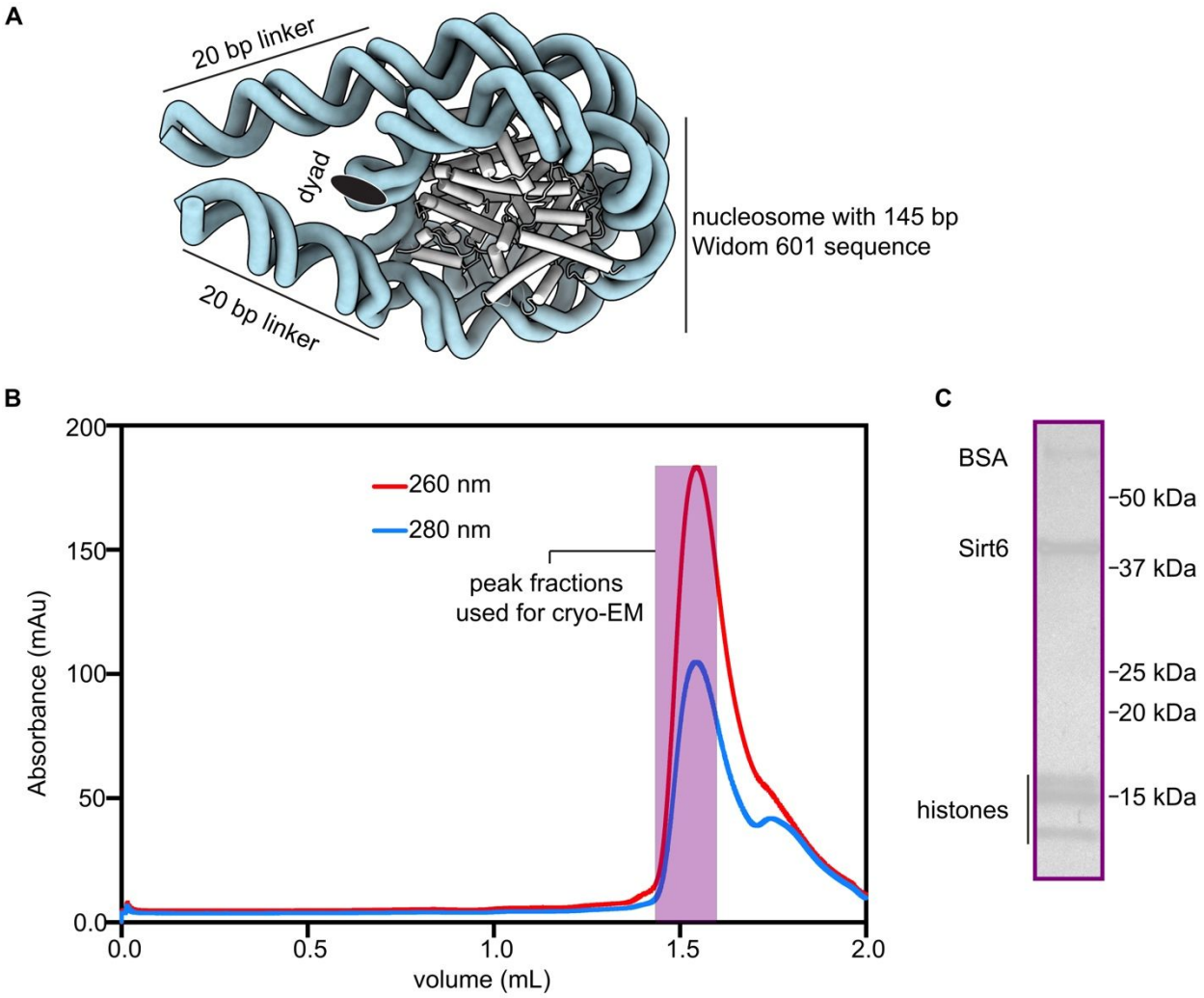

Figure S17. Formation of H3K9MTU nucleosome-Sirt6 complex. (A) Nucleosome structure (B) Chromatogram of nucleosome-Sirt6 complex formation. (C) SDS-PAGE gel of nucleosome-Sirt6 complex.

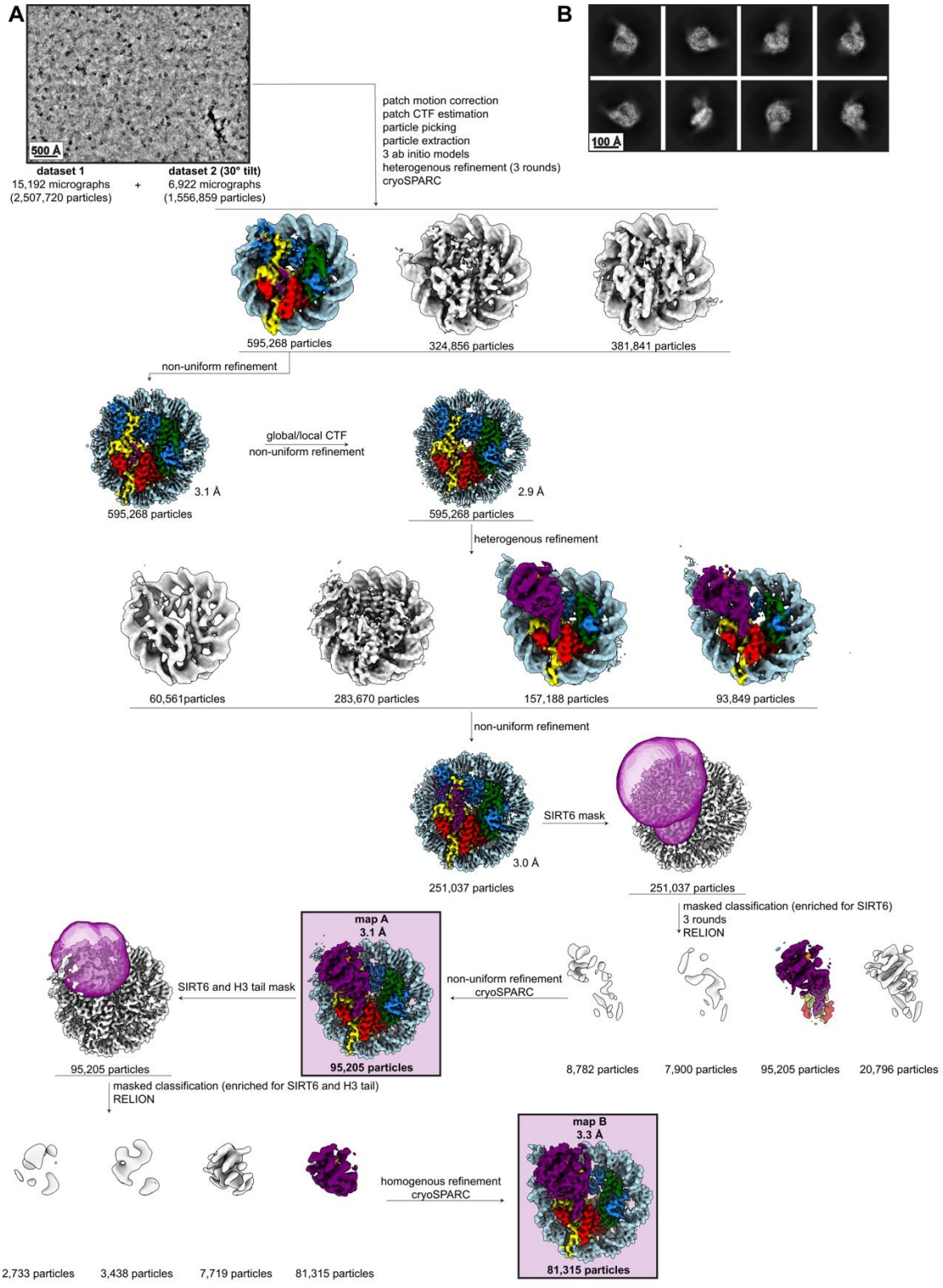

Figure S18. Data acquisition and processing of the nucleosome-Sirt6 complex. (A) Representative low-pass filtered micrograph of data collection with scale bar (500 Å) and sorting and classification tree of nucleosome-Sirt6 complex dataset. Final maps (map A and B) are indicated. (B) 2D classes of final refinement show Sirt6, and nucleosome-like shape with scale bar of 100 Å.

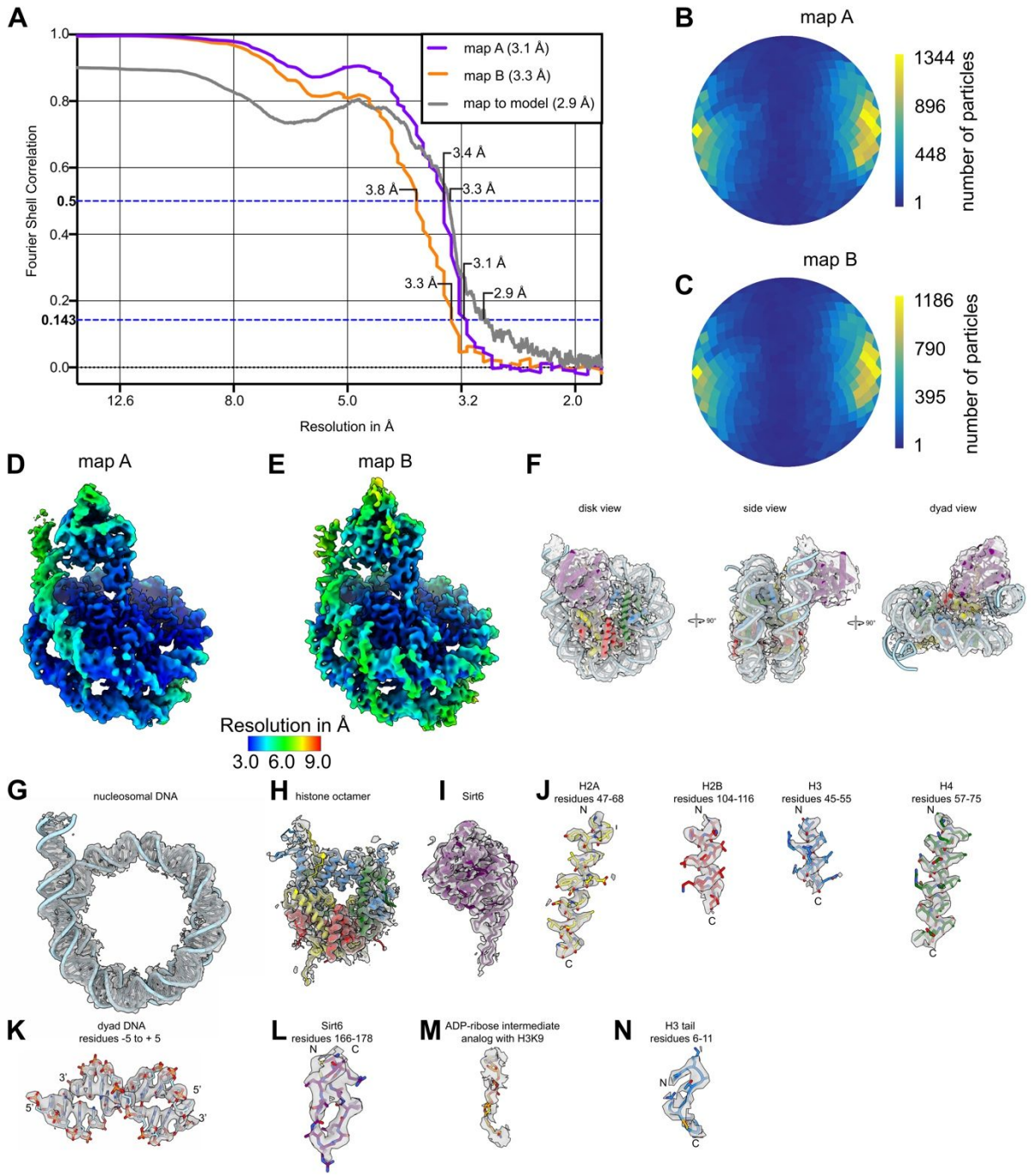

Figure S19. Data quality metrics and densities of the nucleosome-Sirt6 complex. (A) FSC curves of overall maps (map A and B) and map-to-model. Resolutions at FSC threshold criterions 0.143 and 0.5 are indicated. (B,C) Angular distribution of particles employed to reconstruct nucleosome-Sirt6 complex maps A and B. (D,E) Local resolutions of nucleosome-Sirt6 complex maps A and B. (F) Three views of nucleosome-Sirt6 atomic model with corresponding cryo-EM map (map A). Cryo-EM map is shown in grey. (G) DNA with corresponding density from nucleosome-Sirt6 complex (map A). (H) Histone octamer with corresponding density from nucleosome-Sirt6 complex (map A). (I) Sirt6 with corresponding density from nucleosome-Sirt6 complex (map A). (J) Representative histone regions from histone H2A, H2B, H3, and H4 with corresponding density from nucleosome-Sirt6 complex (map A). Residue numbers are indicated. (K) DNA around the dyad (base pairs -5 to +5) with corresponding density from nucleosome-

Sirt6 complex (map A). N- and C-terminus are indicated. (L) Zn binding insertion loop from Sirt6 with corresponding density from nucleosome-Sirt6 complex (map A). Residue numbers are indicated. N- and C-terminus are indicated. (M) NAD transition state analog and H3K9 with corresponding density from nucleosome-Sirt6 complex (map A). (N) H3 tail residues (residues 6-11) with corresponding density from nucleosome-Sirt6 complex (map A). N- and C-terminus are indicated.

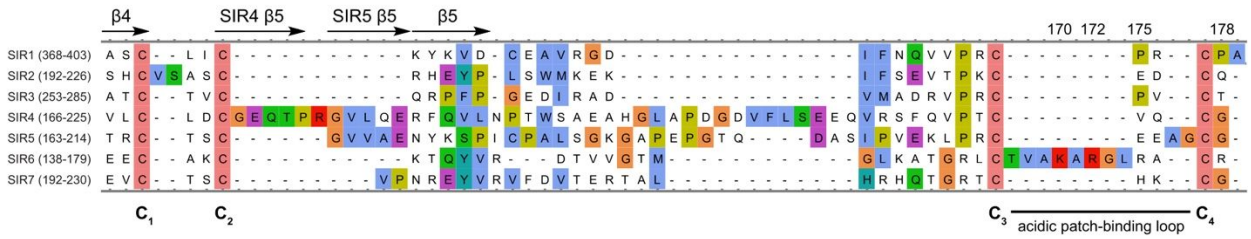

Figure S20. Multiple sequence alignment of *H. sapiens* Sirt1-7 small zinc binding domains. Beta sheets 4 and 5 of the small zinc binding domain are indicated above. Zinc-binding cysteine residues are indicated below. The basic loop involved in Sirt6 binding to the H2A/H2B acidic patch, indicated on the lower right, is unique to Sirt6 among human sirtuins. Basic loop residues are numbered on the top right.

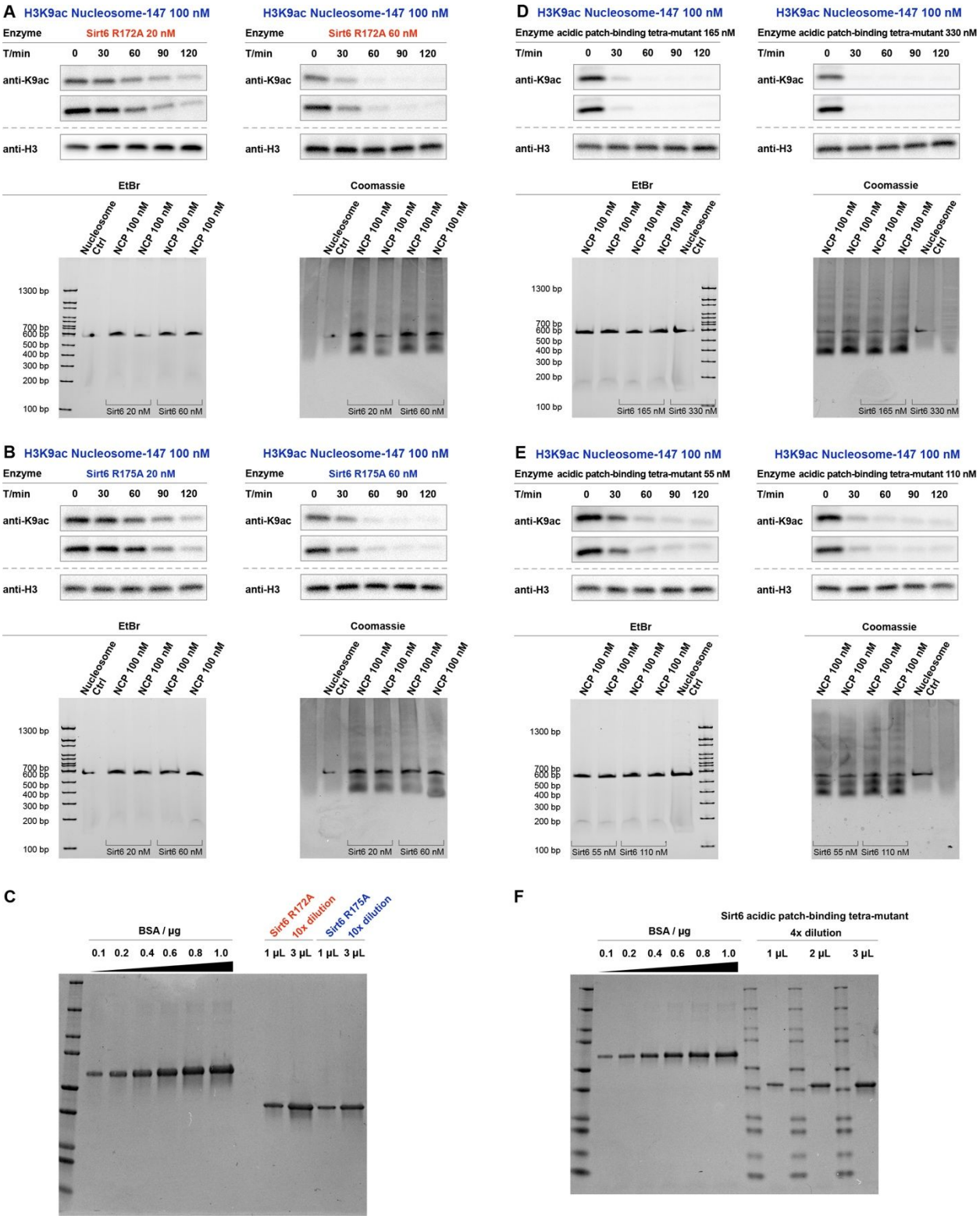

Figure S21. Western blot and curve fitting for deacylation by 3 acidic-patch binding mutants. Western blot of deacetylation assay on H3K9ac nucleosome-147 with (A) Sirt6 R172A (20 nM and 60 nM). (B) Sirt6 R175A (20 nM and 60 nM). (D)(E) Sirt6 acidic patch-binding tetra-mutant (55, 110, 165, and 330 nM). SDS-PAGE densitometry for (C) Sirt6 R172A and Sirt6 R175A; (F) Sirt6 acidic patch-binding tetra-mutant.

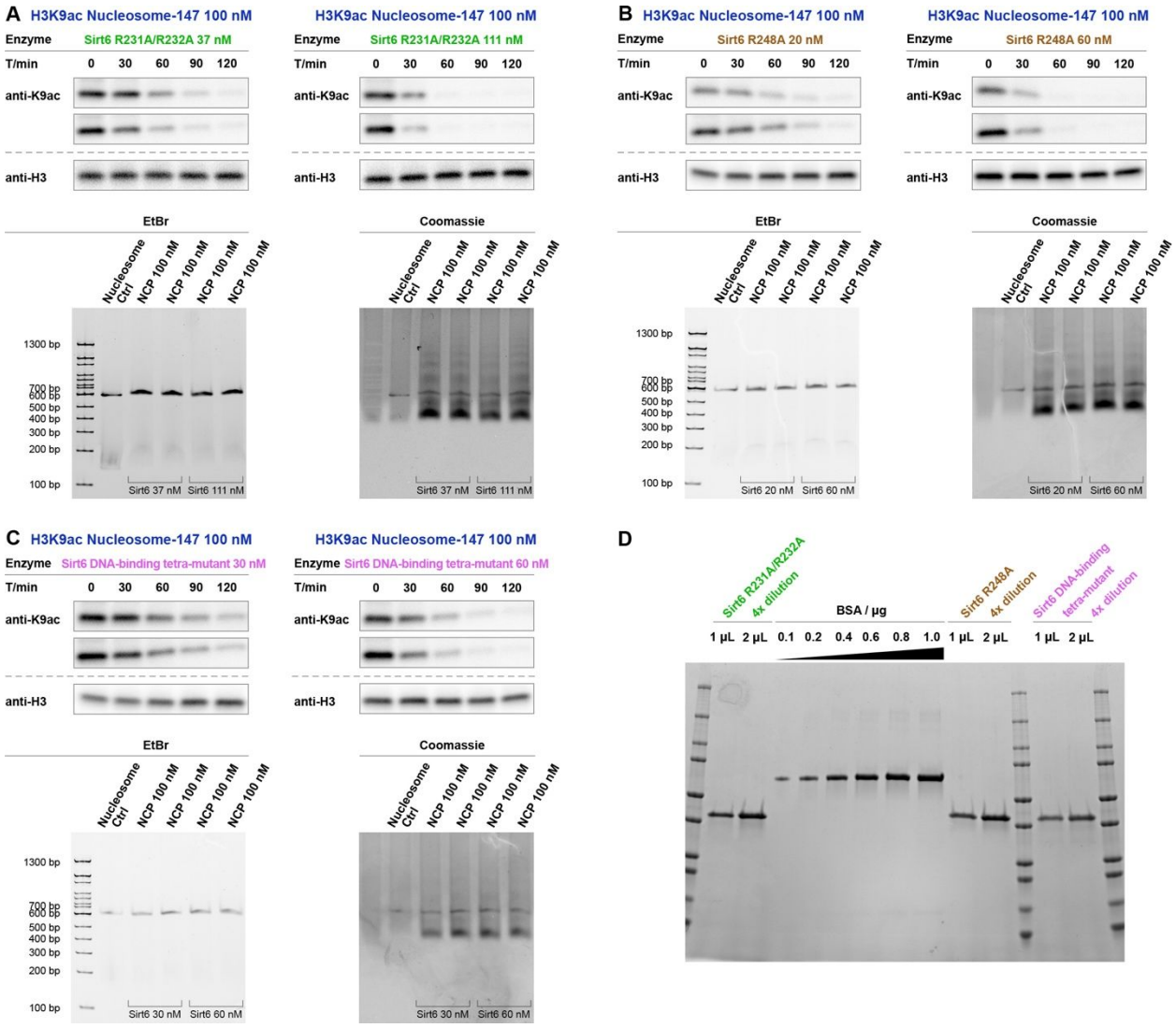

Figure S22. Western blot and curve fitting for deacylation by 3 DNA binding mutants. Western blot of deacetylation assay on H3K9ac nucleosome-147 with (A) Sirt6 R231A/R232A (37 nM and 111 nM). (B) Sirt6 R248A (20 nM and 60 nM). (C) Sirt6 DNA-binding tetra-mutant (30 nM and 60 nM). SDS-PAGE densitometry for (D) Sirt6 R231A/R232A, Sirt6 R248A, and Sirt6 DNA-binding tetra-mutant.

A H3K9ac Nucleosome-185 + WT Sirt6

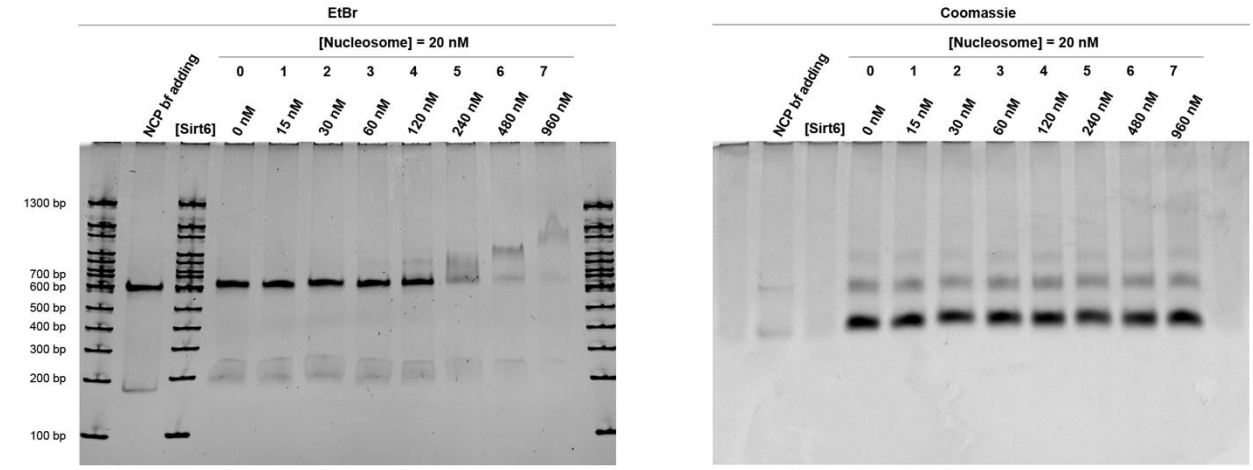

B H3K9ac Nucleosome-185 + WT Sirt6

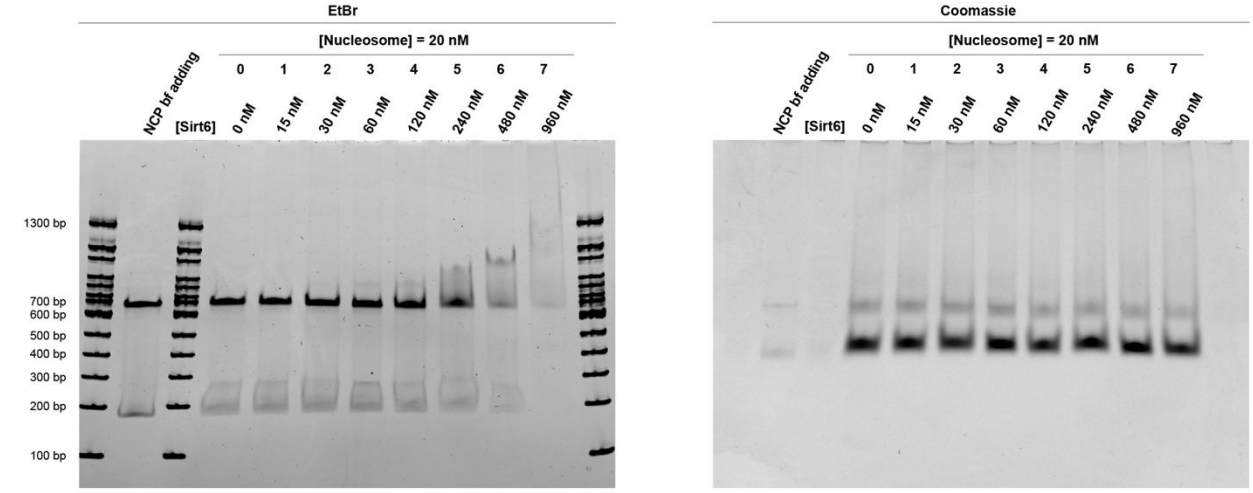

C H3K9ac Nucleosome-185 + Sirt6 R172A

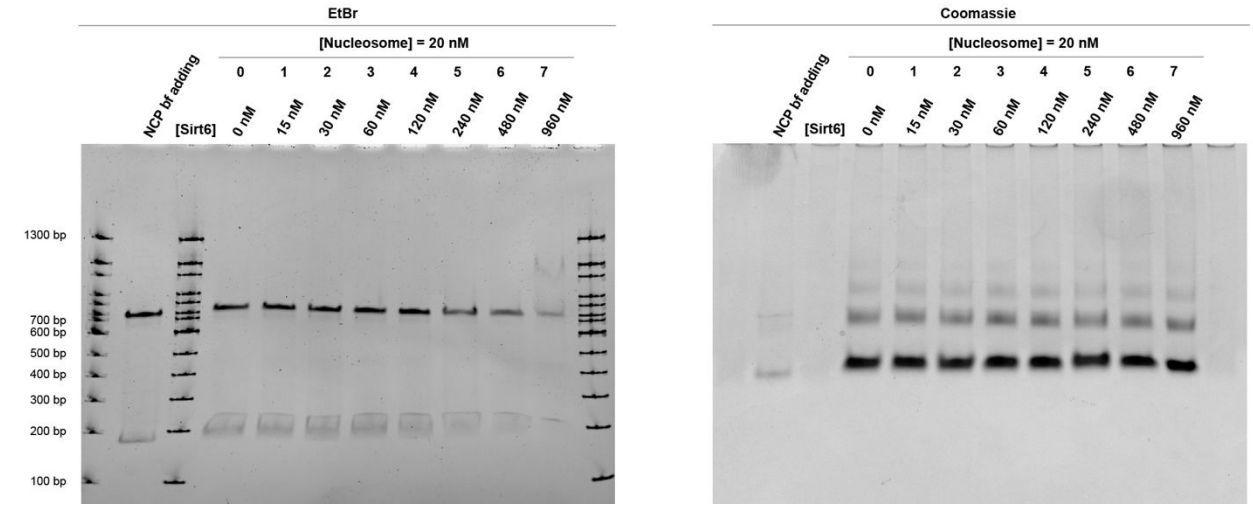

D H3K9ac Nucleosome-185 + Sirt6 R172A

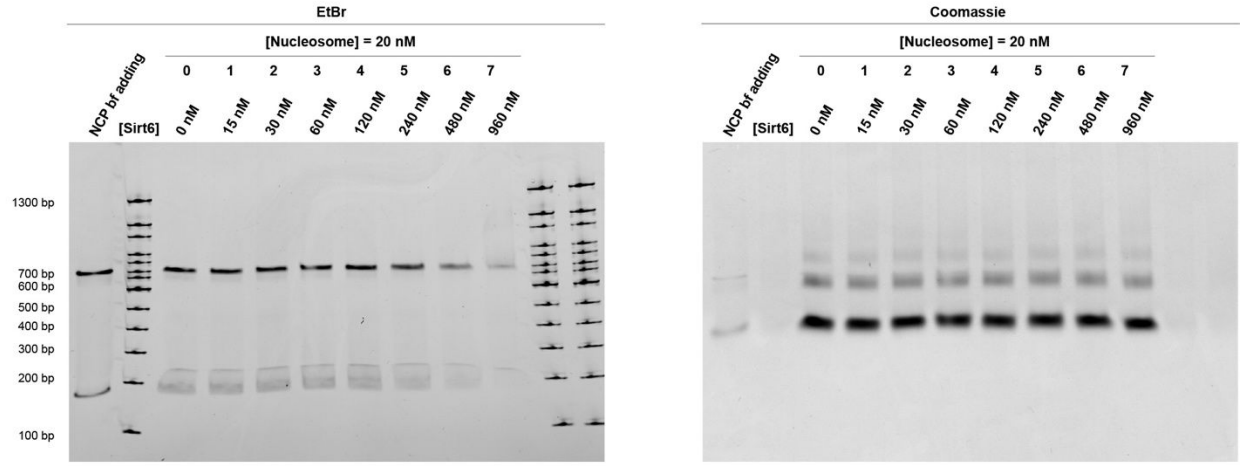

E H3K9ac Nucleosome-185 + Sirt6 R172A

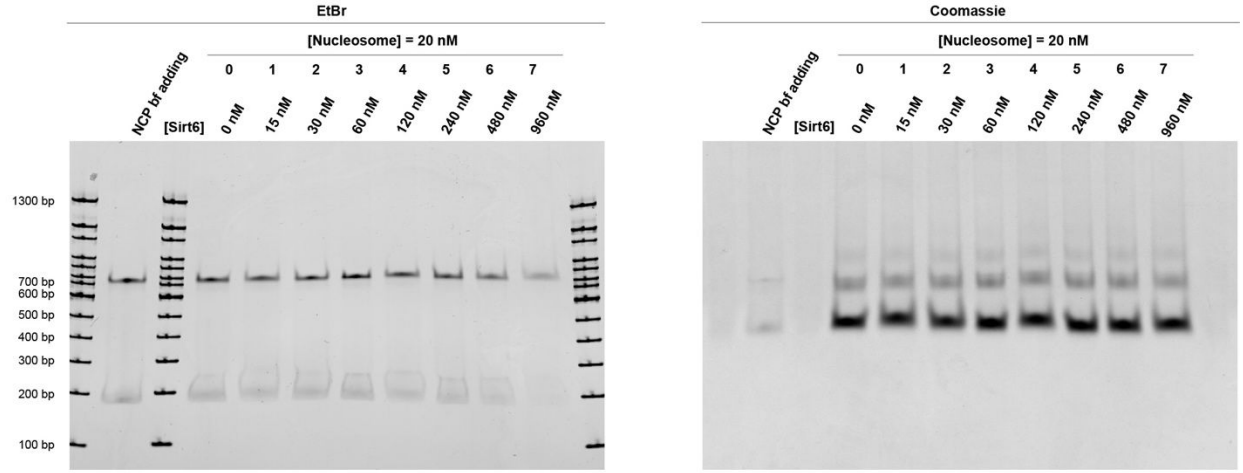

F H3K9ac Nucleosome-185 + Sirt6 R175A

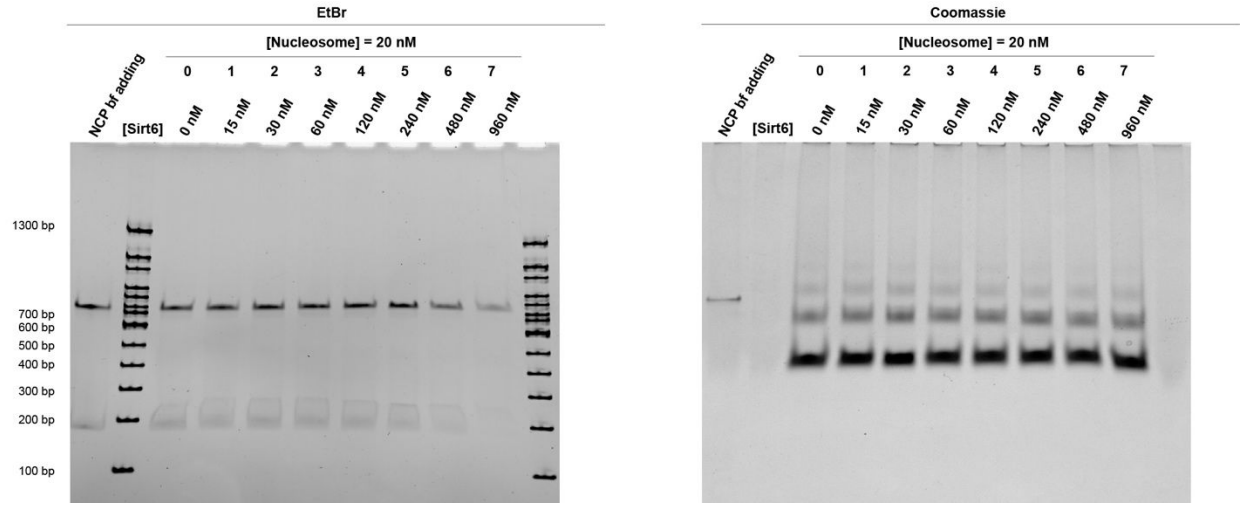

G H3K9ac Nucleosome-185 + Sirt6 R175A

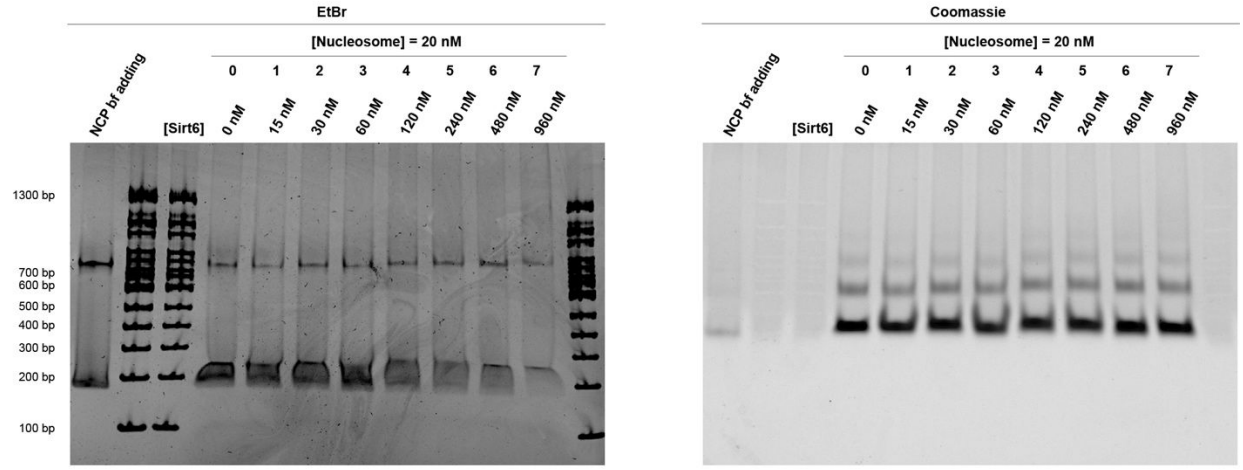

H H3K9ac Nucleosome-185 + Sirt6 acidic patch-binding tetra-mutant

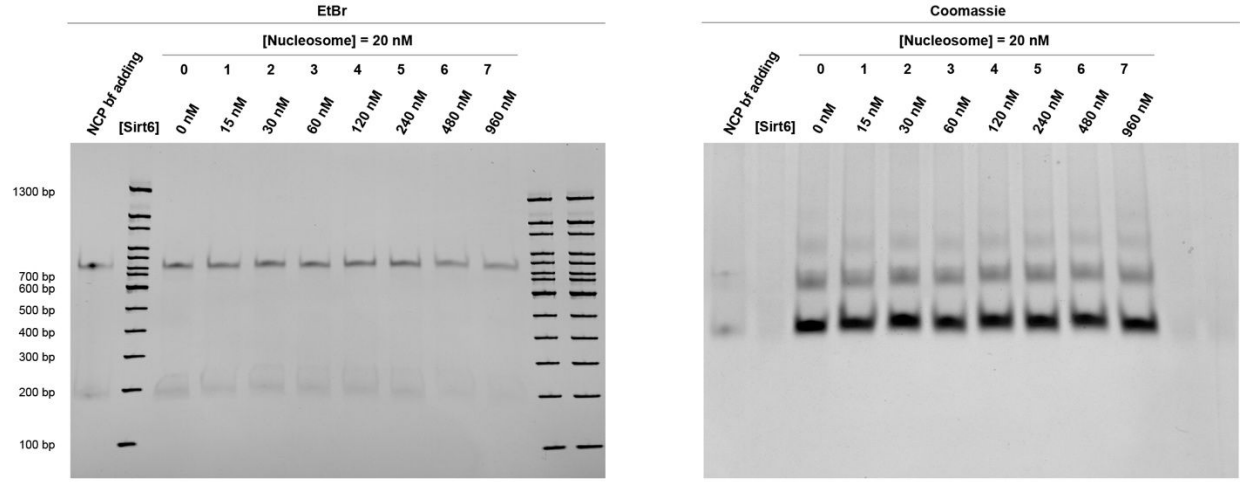

I H3K9ac Nucleosome-185 + Sirt6 acidic patch-binding tetra-mutant

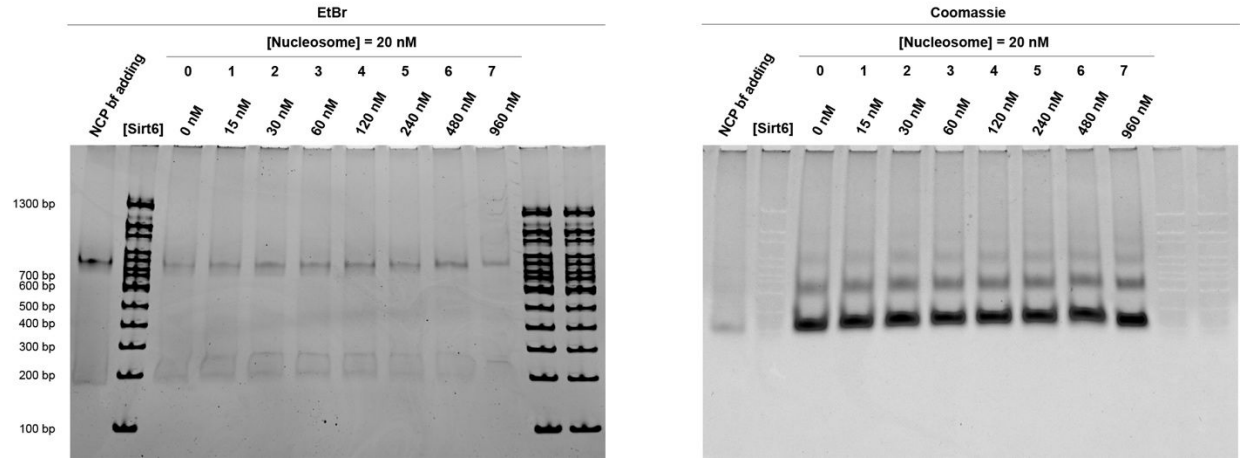

J H3K9ac Nucleosome-185 + Sirt6 R231A/R232A

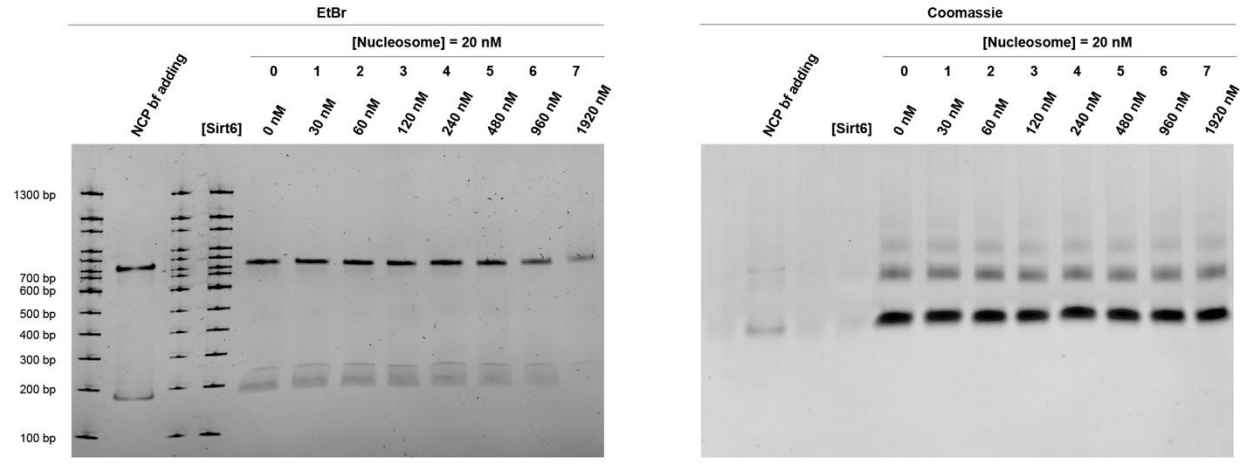

K H3K9ac Nucleosome-185 + Sirt6 R231A/R232A

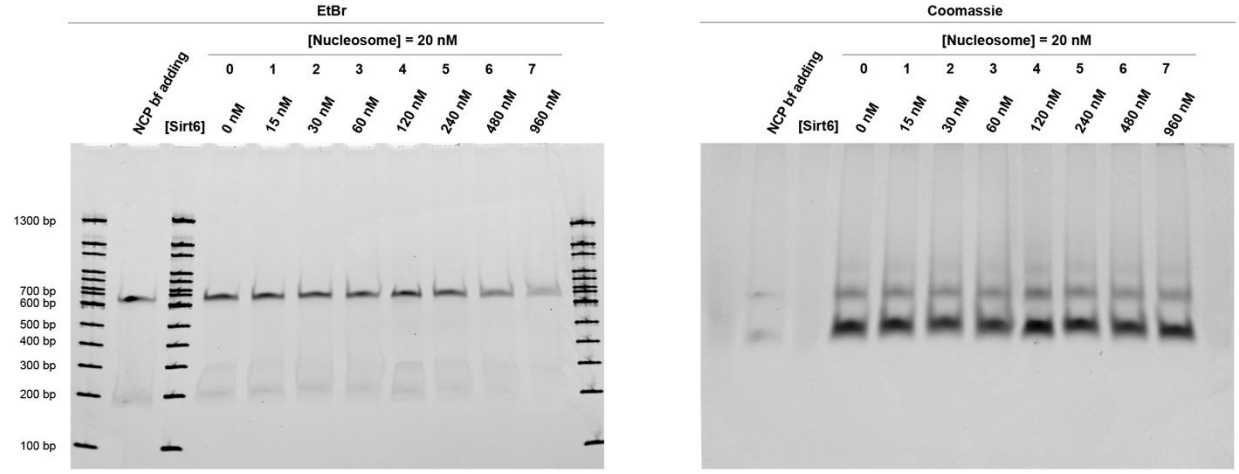

L H3K9ac Nucleosome-185 + Sirt6 R231A/R232A

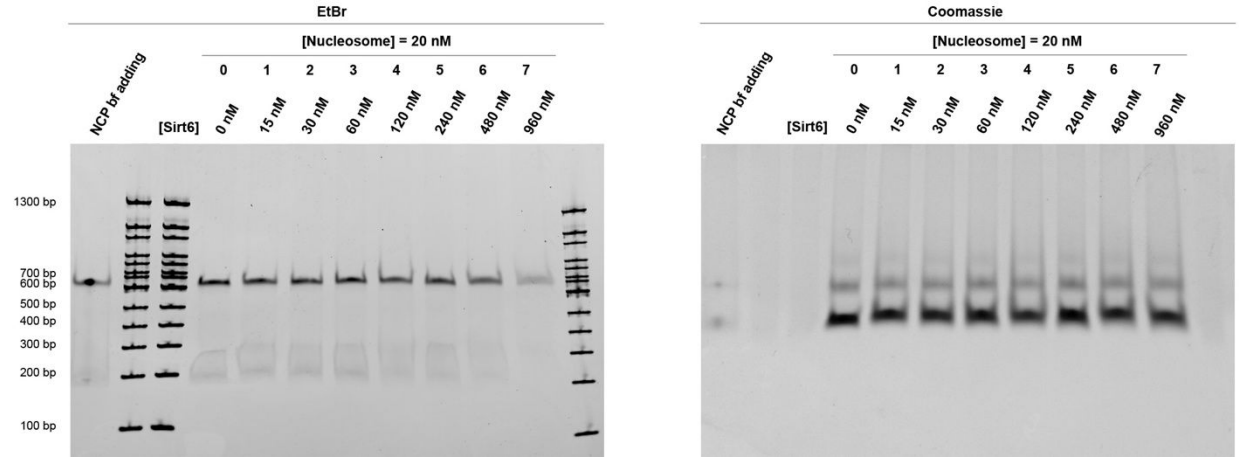

M H3K9ac Nucleosome-185 + Sirt6 R248A

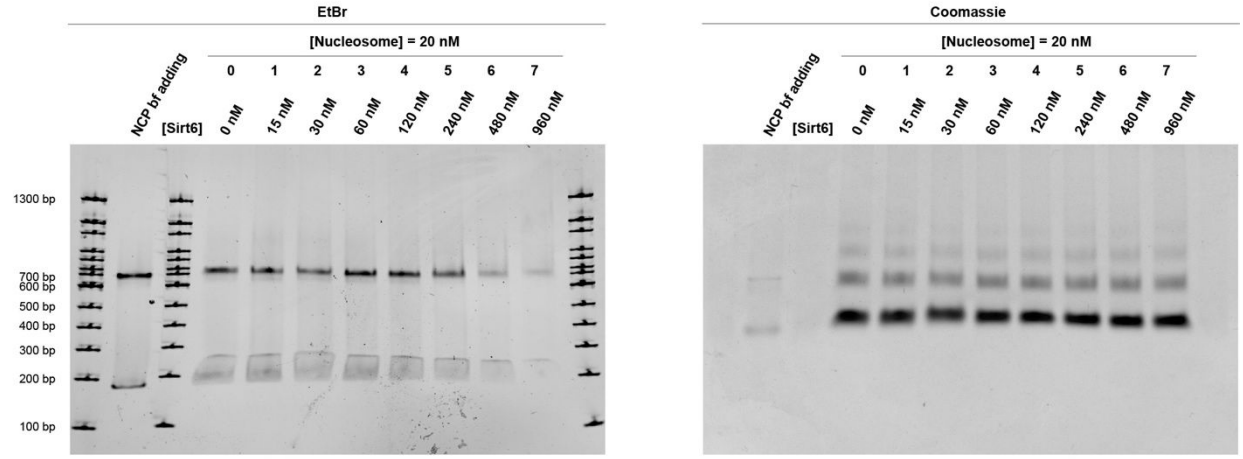

N H3K9ac Nucleosome-185 + Sirt6 R248A

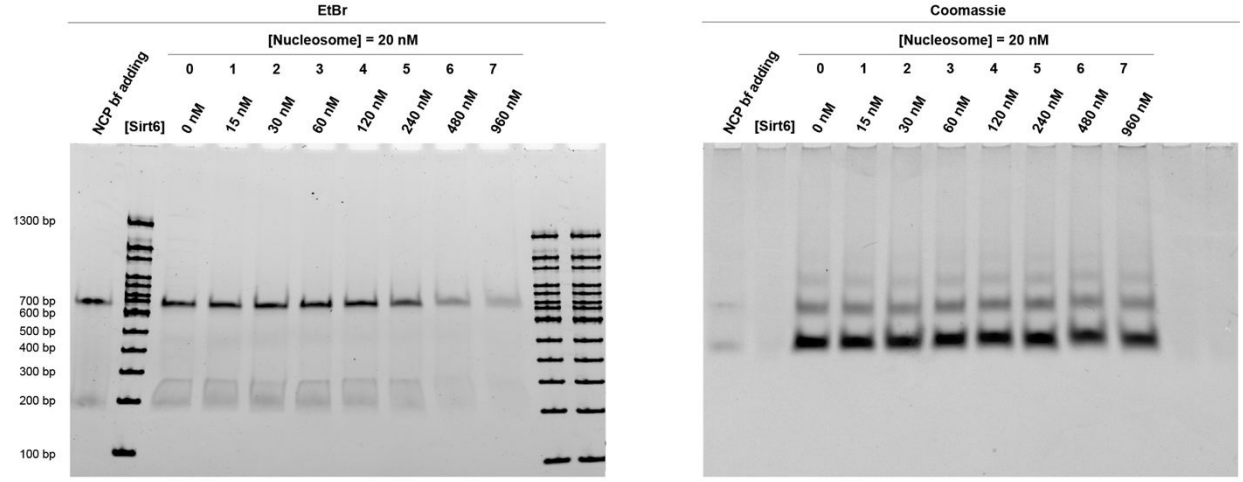

O H3K9ac Nucleosome-185 + Sirt6 DNA-binding tetra-mutant

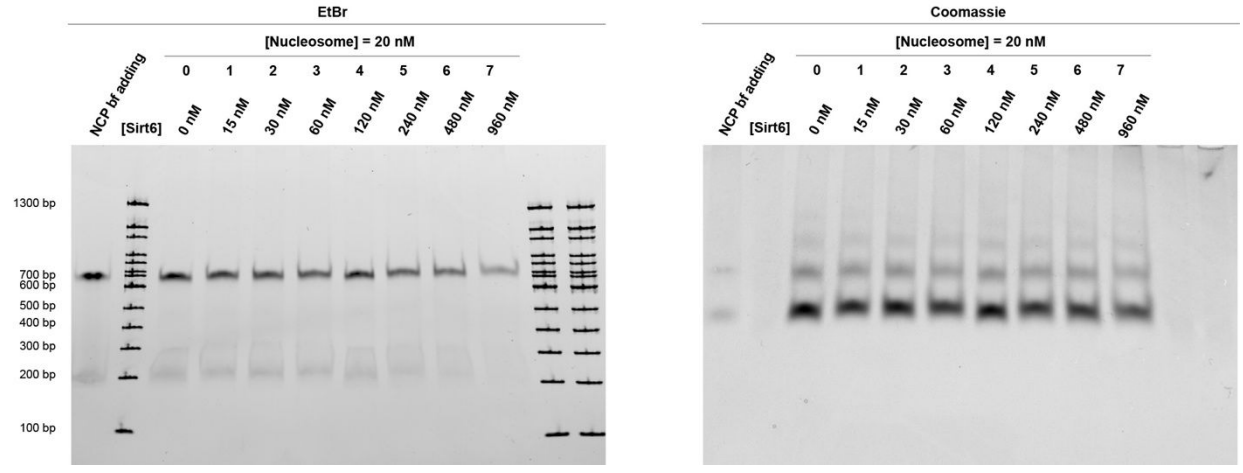

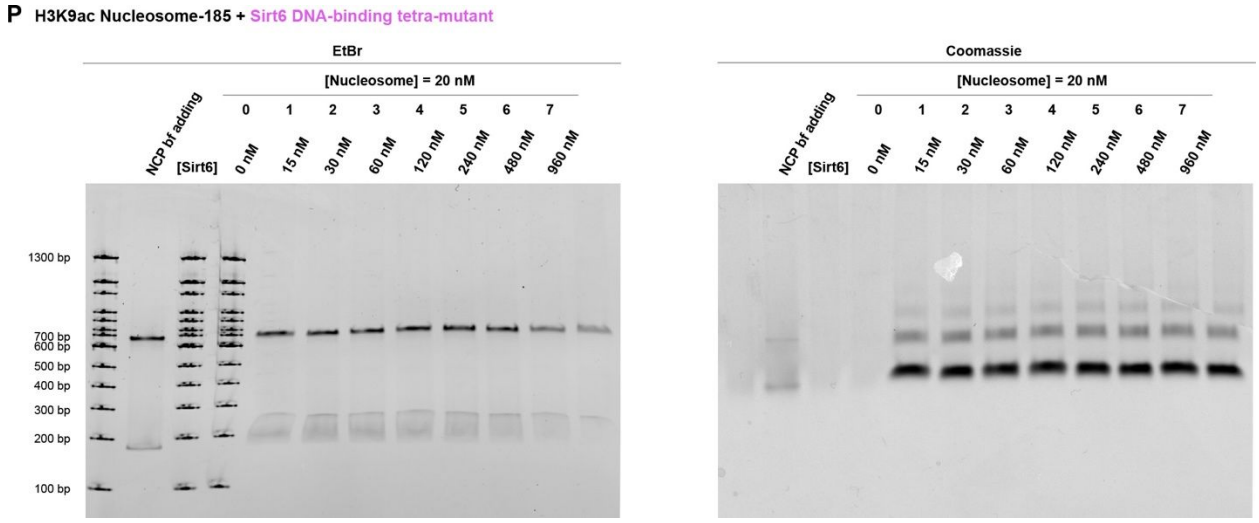

Figure S23. EMSA of WT Sirt6 and Sirt6 mutants with H3K9ac nucleosome-185. EMSA of H3K9ac nucleosome-185 binding with (A)(B) WT Sirt6. (C)(D)(E) Sirt6 R172A. (F)(G) Sirt6 R175A. (H)(I) Sirt6 acidic patch-binding tetra-mutant. (J)(K)(L) Sirt6 R231A/R232A. (M)(N) Sirt6 R248A. (O)(P) Sirt6 DNA-binding tetra-mutant.

Table SI 1-3

Table S1 All the calculated V/[E] for deacetylation assays

H3 Nucleosome sites	V/[E] (min^{-1})		H3 Protein sites	Normalized V/[E] (min^{-1})
H3K9ac	0.10±0.0068		H3K9ac	< 0.01
H3K14ac	0.0012±0.00030		H3K14ac	< 0.01
H3K18ac	0.043±0.0031		H3K18ac	< 0.01
H3K23ac	0.011±0.00059		H3K23ac	< 0.01
H3K27ac	0.040±0.0036		H3K27ac	< 0.01
H2B Nucleosome sites	**V/[E] (min^{-1})**		**H2B Protein sites**	**Normalized V/[E] (min^{-1})**
H3K9ac	0.10±0.068		H3K9ac	< 0.01
H2BK11ac	< 0.001		H2BK11ac	< 0.01
H2BK12ac	< 0.001		H2BK12ac	< 0.01
H2BK20ac	< 0.001		H2BK20ac	< 0.01
H2BK46ac	< 0.001		H2BK46ac	< 0.01
NAD (μM)	**V/[E] (min^{-1})**		**NaCl (mM)**	**V/[E] (min^{-1})**
0	0		0	0.10±0.010
56.95	0.030±0.0053		25	0.15±0.0089
227.8	0.076±0.0065		50	0.071±0.0042
1000	0.102±0.010		100	0.023±0.0015
1139	0.0997±0.0068		250	0.00077±0.00061
Nucleosome-147 (nM)	**V/[E] (min^{-1})**		**Nucleosome-185 (nM)**	**V/[E] (min^{-1})**
0	0		0	0
10	0.053±0.0072		10	0.065±0.0043
20	0.054±0.0096		20	0.058±0.0033
50	0.096±0.012		50	0.093±0.012
100	0.10±0.0048		100	0.11±0.0099
200	0.115±0.011		200	0.13±0.017
400	0.111±0.0057			
log[MDL-800(nM)]	**V_0/V_m**		**Sirt6 mutants**	**V/[E] (min^{-1})**
5	4.1±0.80		R172A	0.057±0.0049
4	3.6±0.57		R175A	0.048±0.0050
3	1.8±0.38		acidic patch-binding tetra-mutant	0.044±0.0020
2	1.5±0.39		R231A/R232A	0.046±0.0062
1	1.6±0.25		R248A	0.060±0.0038
0	1.0±0.19		DNA-binding tetra-mutant	0.038±0.0033

Table S2 Cryo-EM data collection, refinement, and validation statistics

	Sirt6-nucloeosome (map A) PDB 8F86 EMDB 28915	Sirt6-nucleosome (map B)
Data collection and processing		
Magnification	105,000	105,000
Voltage (kV)	300	300
Electron exposure (e^{-}/Å^2)	50.45	50.45
Defocus range (μm)	0.7-1.7	0.7-1.7
Pixel size (Å)	0.83	0.83
Symmetry imposed	C1	C1
Initial particles images (no.)	4,064,579	4,064,579
Final particle images (no.)	95,205	81,315
Map resolution (Å) FSC threshold	3.1 0.143	3.3 0.143
Map resolution range (Å)	3-6	3-8
Refinement		
Initial models used (PDB code)	3LZ0, 5Y2F	
Map sharpening *B* factor (Å^2)	-69.3	-52.3
Model composition		
Non-hydrogen atoms Protein residues Nucleotides Ligands	14400 1054 296 LIG: 1 ZN: 1	
B factors (Å^2) Protein Nucleotide Ligand	124.09 186.18 145.68	
R.m.s. deviations		
Bond lengths (Å) Bond angles (°)	0.004 (0) 0.638 (4)	
Validation		
MolProbity score Clashscore Poor rotamers (%)	1.78 7.47 0.00	
Ramachandran plot		
Favored (%) Allowed (%) Disallowed (%)	94.67 5.14 0.19	

Table S3 Input structural models and confidence

Domain/complex	Chain id	Input model	Level of confidence
Nucleosome	A-J	3LZ0	Atomic, side chains resolved
H2A	C,G	3LZ0	Atomic, side chains resolved
H2B	D,H	3LZ0	Atomic, side chains resolved
H3	A,E	3LZ0,5Y2F	Atomic, side chains resolved
H3 tail (residues 3-13)	A	5Y2F	Atomic, side chains resolved
H4	B,F	3LZ0	Atomic, side chains resolved
DNA	I,J	3LZ0	Atomic, phosphate backbone resolved
SIRT6	K	5Y2F, AlphaFold2	Atomic, rigid body docked, AlphaFold2 modeled; partially side chains resolved or clear secondary structures resolved
SIRT6 (residues 2-16)	K	AlphaFold2	Rigid Body docked
SIRT6 (residues 17-83)	K	5Y2F	Rigid body docked
NAD analog	A	5Y2F	Rigid Body docked, density matches shape